

# Algebraic Models of Hadron Structure

## II. Strange Baryons

R. Bijker

Instituto de Ciencias Nucleares, U.N.A.M.,  
A.P. 70-543, 04510 México D.F., México

F. Iachello

Center for Theoretical Physics, Sloane Laboratory,  
Yale University, New Haven, CT 06520-8120, U.S.A.

A. Leviatan

Racah Institute of Physics, The Hebrew University,  
Jerusalem 91904, Israel

April 3, 2000

### Abstract

The algebraic treatment of baryons is extended to strange resonances. Within this framework we study a collective string-like model in which the radial excitations are interpreted as rotations and vibrations of the strings. We derive a mass formula and closed expressions for strong and electromagnetic decay widths and use these to analyze the available experimental data.

PACS numbers: 14.20.Jn, 13.30.Eg, 13.40.Hq, 03.65.Fd

Annals of Physics (N.Y.), in press

# 1 Introduction

In the last few years there has been renewed interest in hadron spectroscopy. Especially the development of dedicated experimental facilities to probe the structure of hadrons in the nonperturbative region of QCD with far greater precision than before has generated a considerable amount of experimental and theoretical activity [1]. This has stimulated us to reexamine hadron spectroscopy in a novel approach in which both internal (spin-flavor-color) and space degrees of freedom of hadrons are treated algebraically. The new ingredient is the introduction of a space symmetry or spectrum generating algebra for the radial excitations which for mesons was taken as  $U(4)$  [2] and for baryons as  $U(7)$  [3]. The algebraic approach unifies the harmonic oscillator quark model,  $U(4) \supset U(3)$  for mesons and  $U(7) \supset U(6)$  for baryons, with collective string-like models of hadrons.

In the first paper of this series [3] we have introduced  $U(7)$  to study the properties of nonstrange baryons, such as the mass spectrum, electromagnetic couplings [4] and strong decays [5]. In this article we extend these studies to hyperons and present a systematic study of both nonstrange and strange baryons in the framework of a collective string-like  $qqq$  model in which the orbital excitations are treated as rotations and vibrations of the strings. The algebraic structure of the model enables us to obtain transparent results (mass formula, selection rules and decay widths for strong and electromagnetic couplings) that can be used to analyze and interpret the experimental data, and look for evidence of the existence of unconventional (*i.e.* non  $qqq$ ) configurations of quarks and gluons, such as hybrid quark-gluon states  $qqq-g$  or multiquark meson-baryon bound states  $qqq-q\bar{q}$ .

In particular, we discuss the mass spectrum (Sects. 3-4), the strong (Sects. 5-6) and electromagnetic (Sects. 7-8) decay widths. We do this in a framework in which spin-flavor symmetry is broken in a diagonal way in the masses (*i.e.* through a dynamic symmetry). This assumption appears to be sufficient to describe most observables. The breaking of spin-flavor symmetry in hyperon decays can be investigated using a procedure similar to that in Ref. [4] for nonstrange baryons. The results of such a study will be published separately.

## 2 Algebraic models of baryons

We consider baryons to be built of three constituent parts which are characterized by both internal and spatial degrees of freedom.

### 2.1 Degrees of freedom

The internal degrees of freedom of these three parts are taken to be: flavor-triplet  $u, d, s$  (for the light quark flavors), spin-doublet  $S = 1/2$ , and color-triplet. The internal algebraic structure of the constituent parts consists of the usual spin-flavor and color algebras

$$\mathcal{G}_i = SU_{\text{sf}}(6) \otimes SU_c(3) . \quad (2.1)$$

In [3] we discussed various algebraic models of baryons. These models share a common spin-flavor structure (see Eq. (2.1)), but differ in their treatment of radial excitations. Here we consider a collective string-like model with the configuration depicted in Fig. 1. The relevant degrees of freedom for the

relative motion of the three constituent parts of this configuration are provided by the relative Jacobi coordinates which we choose as [6]

$$\begin{aligned}\vec{\rho} &= \frac{1}{\sqrt{2}}(\vec{r}_1 - \vec{r}_2), \\ \vec{\lambda} &= \frac{1}{\sqrt{m_1^2 + m_2^2 + (m_1 + m_2)^2}}[m_1\vec{r}_1 + m_2\vec{r}_2 - (m_1 + m_2)\vec{r}_3].\end{aligned}\quad (2.2)$$

Here  $m_i$  and  $\vec{r}_i$  ( $i = 1, 2, 3$ ) denote the mass and coordinate of the  $i$ -th constituent. When two of the constituents have equal mass ( $m_1 = m_2$ ), the above choice reduces to

$$\begin{aligned}\vec{\rho} &= \frac{1}{\sqrt{2}}(\vec{r}_1 - \vec{r}_2), \\ \vec{\lambda} &= \frac{1}{\sqrt{6}}(\vec{r}_1 + \vec{r}_2 - 2\vec{r}_3).\end{aligned}\quad (2.3)$$

Since the quark masses satisfy to a good approximation  $m_u = m_d \neq m_s$ , the Jacobi coordinates of Eq. (2.3) are relevant for all baryons be it with strangeness  $S = 0, -1, -2$  or  $-3$ . Instead of a formulation in terms of coordinates and momenta, we use the method of bosonic quantization in which we introduce a dipole boson with  $L^P = 1^-$  for each independent relative coordinate, and an auxiliary scalar boson with  $L^P = 0^+$  [3]

$$b_{\rho,m}^\dagger, b_{\lambda,m}^\dagger, s^\dagger \quad (m = -1, 0, 1). \quad (2.4)$$

The scalar boson does not represent an independent degree of freedom, but is added under the restriction that the total number of bosons  $N$  is conserved. This procedure leads to a compact spectrum generating algebra for the radial (or orbital) excitations

$$\mathcal{G}_r = U(7). \quad (2.5)$$

The  $U(7)$  algebra enlarges the  $U(6)$  algebra of the harmonic oscillator quark model [7], but still describes the dynamics of two vectors. For a system of interacting bosons the model space is spanned by the symmetric irreducible representation  $[N]$  of  $U(7)$ . This representation contains all oscillator shells with  $n = n_\rho + n_\lambda = 0, 1, 2, \dots, N$ . The value of  $N$  determines the size of the model space and, in view of confinement, is expected to be large.

## 2.2 Basis states

The full algebraic structure is obtained by combining the spatial part  $\mathcal{G}_r$  of Eq. (2.5) with the internal spin-flavor-color part  $\mathcal{G}_i$  of Eq. (2.1)

$$\mathcal{G} = \mathcal{G}_r \otimes SU_{\text{sf}}(6) \otimes SU_c(3). \quad (2.6)$$

The spatial part of the baryon wave function has to be combined with the spin-flavor and color part, in such a way that the total wave function is antisymmetric. Since the color part of the wave function is antisymmetric (color singlet), the remaining part (space-spin-flavor) has to be symmetric. A convenient set of basis states is provided by the case of three identical constituents, for which the spatial and spin-flavor parts of the baryon wave function are in addition labeled by their transformation properties under

the permutation group  $S_3$ :  $t = S$  for the symmetric,  $t = A$  for the antisymmetric and  $t = M$  for the two-dimensional ( $M_\rho, M_\lambda$ ) mixed symmetry representation.

A set of basis states for the spin-flavor part is provided by the decomposition of  $SU_{\text{sf}}(6)$  into its flavor and spin parts

$$\left| \begin{array}{cccccc} SU_{\text{sf}}(6) & \supset & SU_{\text{f}}(3) & \otimes & SU_{\text{s}}(2) & \supset & SU_{\text{I}}(2) & \otimes & U_{\text{Y}}(1) & \otimes & SU_{\text{s}}(2) \\ \downarrow & & \downarrow & & \downarrow & & \downarrow & & \downarrow & & \\ [f_1 f_2 f_3] & & [g_1 g_2] & & S & & I & & Y & & \end{array} \right\}. \quad (2.7)$$

Here  $[f_1 f_2 f_3]$  and  $[g_1 g_2]$  represent the Young tableaux,  $S$  denotes the spin,  $I$  the isospin and  $Y$  the hypercharge. The representations of the spin-flavor groups are often labeled by their dimensions (rather than by their Young tableaux)

$$\begin{aligned} \dim[f_1 f_2 f_3] &= \frac{(f_1 - f_2 + 1)(f_1 - f_3 + 2)(f_2 - f_3 + 1)(f_1 + 5)!(f_2 + 4)!(f_3 + 3)!}{3!4!5!(f_1 + 2)!(f_2 + 1)!f_3!}, \\ \dim[g_1 g_2] &= \frac{1}{2}(g_1 - g_2 + 1)(g_1 + 2)(g_2 + 1), \\ \dim[S] &= 2S + 1. \end{aligned} \quad (2.8)$$

For three constituent parts the allowed values of  $[f_1 f_2 f_3]$  are  $[300]$  ( $t = S$ ),  $[210]$  ( $t = M$ ) and  $[111]$  ( $t = A$ ) with dimensions 56, 70 and 20, respectively. The flavor part is characterized by  $[g_1 g_2] = [30]$ ,  $[21]$  or  $[00]$  with dimensions 10 (decuplet), 8 (octet) or 1 (singlet), respectively. In the notation of [8] the flavor wave functions are labeled by  $(p, q) = (g_1 - g_2, g_2)$ . Finally, the total spin of three spin-1/2 objects is  $S = 3/2$  or  $S = 1/2$ . The decomposition of representations of  $SU_{\text{sf}}(6)$  into those of  $SU_{\text{f}}(3) \otimes SU_{\text{s}}(2)$  is the standard one

$$\begin{aligned} S &\leftrightarrow [56] \supset 2^8 \oplus 4^{10}, \\ M &\leftrightarrow [70] \supset 2^8 \oplus 4^8 \oplus 2^{10} \oplus 2^1, \\ A &\leftrightarrow [20] \supset 2^8 \oplus 4^1, \end{aligned} \quad (2.9)$$

where we have denoted the irreducible representations by their dimensions. Each flavor multiplet consists of families of baryons which are characterized by their isospin  $I$  and hypercharge  $Y$  (see Table I). The electric charge is given by the Gell-Mann and Nishijima relation

$$Q = I_3 + \frac{Y}{2}. \quad (2.10)$$

In Appendix A we present the explicit form for the spin and flavor wave functions in the convention that we have used in this paper.

Since the space-spin-flavor wave function is symmetric ( $t = S$ ), the symmetry of the spatial wave function under  $S_3$  has to be the same as that of the spin-flavor part. Hence it is convenient to label the spatial wave functions by the basis states of a dynamical symmetry of  $U(7)$  that preserves the  $S_3$  permutation symmetry. We choose the chain that corresponds to the problem of three particles in a common harmonic oscillator potential [9]

$$\left| \begin{array}{ccccccc} U(7) & \supset & U(6) & \supset & SU(3) & \otimes & SU(2) & \supset & SO(3) & \otimes & SO(2) \\ N & , & n & , & (n_1, n_2) & , & F & , & L & , & m_F \end{array} \right\}. \quad (2.11)$$

In this decomposition, the behavior in three-dimensional coordinate space  $SU(3) \supset SO(3)$  is separated from that in index space  $SU(2) \supset SO(2)$ . The allowed values of the quantum numbers can be obtained from the branching rules. For the decomposition of  $U(6)$  we use the complementarity relationship between the groups  $SU(3)$  and  $SU(2)$  within the symmetric irreducible representation  $U(6)$ . As a consequence, the labels of  $SU(3)$  are determined by those of  $SU(2)$ . The branching rules are

$$\begin{aligned}
n &= 0, 1, \dots, N, \\
F &= n, n-2, \dots, 1 \text{ or } 0, \\
(n_1, n_2) &= \left( \frac{n+F}{2}, \frac{n-F}{2} \right), \\
m_F &= -F, -F+2, \dots, F.
\end{aligned} \tag{2.12}$$

The reduction from the coupled harmonic oscillator group to the rotation group  $SU(3) \supset SO(3)$  is given by [10]

$$\begin{aligned}
K &= \min\{\lambda, \mu\}, \min\{\lambda, \mu\} - 2, \dots, 1 \text{ or } 0, \\
K = 0 : & \quad L = \max\{\lambda, \mu\}, \max\{\lambda, \mu\} - 2, \dots, 1 \text{ or } 0, \\
K > 0 : & \quad L = K, K+1, \dots, K + \max\{\lambda, \mu\}.
\end{aligned} \tag{2.13}$$

Here  $(\lambda, \mu) = (n_1 - n_2, n_2) = (F, (n-F)/2)$ . The label  $K$  is an extra label that has to be introduced to label the states uniquely [10]. The  $SO(2)$  group in Eq. (2.11) is related to the permutation symmetry [3, 9, 7]. The states with good  $S_3$  symmetry are given by the linear combinations

$$\begin{aligned}
|\psi_1\rangle &= \frac{-i}{\sqrt{2(1 + \delta_{m_F, 0})}} [|\phi_{m_F}\rangle - |\phi_{-m_F}\rangle], \\
|\psi_2\rangle &= \frac{(-1)^\nu}{\sqrt{2(1 + \delta_{m_F, 0})}} [|\phi_{m_F}\rangle + |\phi_{-m_F}\rangle].
\end{aligned} \tag{2.14}$$

Here we have introduced the label  $\nu$  by  $m_F = \nu \pmod{3}$ . The wave functions  $|\psi_1\rangle$  ( $|\psi_2\rangle$ ) transform for  $\nu = 0$  as  $t = A$  ( $S$ ), and for  $\nu = 1, 2$  as  $t = M_\rho$  ( $M_\lambda$ ). Summarizing, the basis states are characterized uniquely by

$$|N, n, F, m_F, K, L_t^P\rangle, \tag{2.15}$$

where  $P$  is the parity of the basis states  $P = (-)^n$ . Finally, the quark orbital angular momentum  $L$  is coupled with the spin  $S$  to the total angular momentum  $J$  of the baryon. In Appendix B we present the space-spin-flavor baryon wave functions with  $S_3$  symmetry.

### 3 Mass operator

The mass operator depends both on the spatial and the internal degrees of freedom. For the spatial part we adopt a collective model of the nucleon in which the baryons are interpreted as rotational and vibrational excitations of the string configuration of Fig. 1. For two identical constituent parts (as is the case for strange baryons) the vibrations are described by [6]

$$\hat{M}_{\text{vib}}^2 = A P_1^\dagger P_1 + B P_2^\dagger P_2 + C P_3^\dagger P_3 + D (P_1^\dagger P_2 + P_2^\dagger P_1), \tag{3.1}$$

with

$$\begin{aligned}
P_1^\dagger &= R^2 s^\dagger s^\dagger - b_\rho^\dagger \cdot b_\rho^\dagger - b_\lambda^\dagger \cdot b_\lambda^\dagger , \\
P_2^\dagger &= (\cos \beta)^2 b_\rho^\dagger \cdot b_\rho^\dagger - (\sin \beta)^2 b_\lambda^\dagger \cdot b_\lambda^\dagger , \\
P_3^\dagger &= b_\rho^\dagger \cdot b_\lambda^\dagger .
\end{aligned} \tag{3.2}$$

Here  $R$  is related to the hyperspherical radius  $\sqrt{\rho^2 + \lambda^2}$ , and  $\beta$  corresponds to the hyperspherical angle  $\tan \beta = \rho/\lambda$  with  $\rho = |\vec{\rho}|$  and  $\lambda = |\vec{\lambda}|$ . The mass operator in this case is  $S_2$  invariant. In the limit of a large model space ( $N \rightarrow \infty$ ) the mass operator of Eqs. (3.1)-(3.2) reduces to leading order in  $N$  to a harmonic form, and its eigenvalues are given by [6]

$$M_{\text{vib}}^2 = \kappa_1 n_u + \kappa_2 n_v + \kappa_3 n_w , \tag{3.3}$$

Here  $\kappa_1, \kappa_2$  are the eigenvalues of the  $2 \times 2$  symmetric matrix

$$\begin{pmatrix} 4ANR^2 & 2DN \sin(2\beta)R^2/\sqrt{1+R^2} \\ 2DN \sin(2\beta)R^2/\sqrt{1+R^2} & BN \sin^2(2\beta)R^2/(1+R^2) \end{pmatrix} . \tag{3.4}$$

and  $\kappa_3 = CNR^2/(1+R^2)$ . The vibrational quantum numbers  $n_u, n_v$  and  $n_w$  denote the number of quanta in the symmetric stretching (or breathing mode), antisymmetric stretching and bending vibrations of the strings, respectively (see Fig. 3 of [3]). For three identical constituents we obtain the  $S_3$ -invariant mass operator of [3] from Eqs. (3.1)-(3.2) by taking  $D = 0, B = C$  and  $\beta = \pi/4$ , which leads to  $\kappa_1 = 4ANR^2$  and  $\kappa_2 = \kappa_3 = BNR^2/(1+R^2)$ . In the analysis of the mass spectrum of strange baryons, to be presented below, the  $S_3$  symmetry of the mass operator is only broken dynamically in the spin-flavor part. Therefore, the baryon wave functions still have good  $S_3$  symmetry, and the vibrational part of the mass operator only depends on  $\kappa_1$  and  $\kappa_2$  for all baryons

$$M_{\text{vib}}^2 = \kappa_1 v_1 + \kappa_2 v_2 . \tag{3.5}$$

Here  $v_1 = n_u$  and  $v_2 = n_v + n_w$  are the vibrational quantum numbers corresponding to the symmetric stretching vibration along the direction of the strings (breathing mode), and two degenerate bending vibrations of the strings. The spectrum consists of a series of vibrational excitations characterized by the labels  $(v_1, v_2)$ , and a tower of rotational excitations built on top of each vibration. The occurrence of linear Regge trajectories suggests to add a term linear in  $L$  to the mass operator

$$M_{\text{space}}^2 = \kappa_1 v_1 + \kappa_2 v_2 + \alpha L . \tag{3.6}$$

In the application to nonstrange baryons [3] the Roper N(1440), the  $\Delta(1600)$  and the  $\Delta(1900)$  resonances were assigned to the symmetric stretching vibration  $(v_1, v_2) = (1, 0)$ , and the N(1710) resonance to the  $(v_1, v_2) = (0, 1)$  vibration. The remaining resonances were interpreted as rotational excitations.

For the spin-flavor part of the mass operator we use the Gürsey-Radicati [11] form

$$\begin{aligned}
\hat{M}_{\text{sf}}^2 &= a \left[ \hat{C}_2(SU_{\text{sf}}(6)) - 45 \right] + b \left[ \hat{C}_2(SU_{\text{f}}(3)) - 9 \right] + c \left[ \hat{C}_2(SU_{\text{s}}(2)) - \frac{3}{4} \right] \\
&+ d \left[ \hat{C}_1(U_{\text{Y}}(1)) - 1 \right] + e \left[ \hat{C}_2(U_{\text{Y}}(1)) - 1 \right] + f \left[ \hat{C}_2(SU_1(2)) - \frac{3}{4} \right] .
\end{aligned} \tag{3.7}$$

The eigenvalues of the Casimir operators in the basis states of Eq. (2.7) are

$$\begin{aligned}
\langle \hat{C}_2(SU_{sf}(6)) \rangle &= 2 \left[ f_1(f_1 + 5) + f_2(f_2 + 3) + f_3(f_3 + 1) - \frac{1}{6}(f_1 + f_2 + f_3)^2 \right] , \\
\langle \hat{C}_2(SU_f(3)) \rangle &= \frac{3}{2} \left[ g_1(g_1 + 2) + g_2^2 - \frac{1}{3}(g_1 + g_2)^2 \right] , \\
\langle \hat{C}_2(SU_s(2)) \rangle &= S(S + 1) , \\
\langle \hat{C}_1(U_Y(1)) \rangle &= Y , \\
\langle \hat{C}_2(U_Y(1)) \rangle &= Y^2 , \\
\langle \hat{C}_2(SU_I(2)) \rangle &= I(I + 1) .
\end{aligned} \tag{3.8}$$

We have defined the operators such that each of the terms vanishes for the ground state of the nucleon. The spin term represents spin-spin interactions, the flavor term denotes the flavor dependence of the interactions, and the  $SU_{sf}(6)$  term, which according to Eq. (3.8) depends on the permutation symmetry of the wave functions, represents ‘signature dependent’ interactions. These signature dependent (or exchange) interactions were extensively investigated years ago within the framework of Regge theory [12]. The last two terms represent the isospin and hypercharge dependence of the masses. We do not consider here interaction terms that mix the space and internal degrees of freedom.

## 4 Comparison with experimental mass spectrum

In this section we analyze simultaneously the experimental mass spectrum of strange and nonstrange baryons in terms of the mass formula

$$\begin{aligned}
M^2 &= M_0^2 + \kappa_1 v_1 + \kappa_2 v_2 + \alpha L \\
&+ a \left[ 2f_1(f_1 + 5) + 2f_2(f_2 + 3) + 2f_3(f_3 + 1) - \frac{1}{3}(f_1 + f_2 + f_3)^2 - 45 \right] \\
&+ b \left[ \frac{3}{2} \left( g_1(g_1 + 2) + g_2^2 - \frac{1}{3}(g_1 + g_2)^2 \right) - 9 \right] + c \left[ S(S + 1) - \frac{3}{4} \right] \\
&+ d \left[ Y - 1 \right] + e \left[ Y^2 - 1 \right] + f \left[ I(I + 1) - \frac{3}{4} \right] .
\end{aligned} \tag{4.1}$$

The coefficient  $M_0^2$  is determined by the nucleon mass  $M_0^2 = 0.882 \text{ GeV}^2$ . The remaining nine coefficients are obtained in a simultaneous fit to the three and four star resonances of Tables III and IV which have been assigned as octet and decuplet states. We find a good overall fit for 48 resonances with an r.m.s. deviation of  $\delta = 33 \text{ MeV}$ . The values of the parameters are given in Table II. In the last column we show for comparison the parameters that were obtained in a fit to 25 nucleon and delta resonances with a r.m.s. deviation to  $\delta = 39 \text{ MeV}$  [3]. In comparison with Table II of [3] the  $\Delta(1900)S_{31}$  was left out, since it has been downgraded from a three to a two star resonance [13]. Since for nonstrange resonances  $Y = 1$ , the  $d$  and  $e$  terms in Eq. (4.1) do not contribute. The flavor and isospin dependent terms that determine the mass splitting between the nucleon and  $\Delta$  resonances can be combined into a single  $b$  term with strength  $b + \frac{1}{3}f = 0.031 \text{ GeV}^2$ , very close to the fitted value of  $0.030 \text{ GeV}^2$  for nonstrange baryons. Thus, the parameter values determined in the present simultaneous study of both strange and nonstrange resonances are almost the same as those found for nonstrange resonances.

Tables III and IV and Figs. 3–6 show that the mass formula of Eq. (4.1) provides a good overall description of both positive and negative baryon resonances belonging to the  $N$ ,  $\Delta$ ,  $\Sigma$ ,  $\Lambda$ ,  $\Xi$  and  $\Omega$  families. There is no need for an additional energy shift for the positive parity states and another one for the negative parity states, as in the relativized quark model [14].

#### 4.1 Octet and decuplet resonances

The results are presented in Fig. 2 for the ground state baryon octet with  $J^P = 1/2^+$  and the baryon decuplet with  $J^P = 3/2^+$ . In Tables III and IV we show a comparison with all three and four star resonances. In our calculation we have assigned the  $N(1440)$ ,  $\Delta(1600)$ ,  $\Sigma(1660)$  and  $\Lambda(1600)$  resonances to the vibration characterized by  $(v_1, v_2) = (1, 0)$ , and the  $N(1710)$ ,  $\Sigma(1940)$  and  $\Lambda(1810)$  resonances to the  $(v_1, v_2) = (0, 1)$  vibration. The remaining resonances are assigned as rotational members of the ground band with  $(v_1, v_2) = (0, 0)$ .

We have followed the quark model assignments of Table 13.4 of [13], with the exception of the  $\Sigma(1750)S_{11}$  resonance which we have assigned as  ${}^28_{1/2}[70, 1^-]$ , the lowest  $S_{11}$  state with a mass of 1711 MeV. In our calculation the lowest four  $S_{11}$   $\Sigma$  states occur at 1711, 1755, 1822 and 1974 MeV (for the assignments we refer to Tables V and VI; the second state belongs to the decuplet). In the nucleon and  $\Lambda$  families the Roper resonance lies below the first excited negative parity resonance. We expect the same to be true for the  $\Sigma$  hyperons. With our assignment,  $\Sigma(1750)$  is the octet partner of  $N(1535)$  and  $\Lambda(1670)$ , which is also supported by their  $\eta$  decay properties [15, 16]. In [13] the two star  $\Sigma(1620)$  resonance has been assigned as the  ${}^28_{1/2}[70, 1^-]$  state, and the  $\Sigma(1750)$  resonance instead as the  ${}^48_{1/2}[70, 1^-]$  state. Our assignment of  $\Sigma(1750)$  coincides with that of [17]. In the relativized quark model there are three low-lying  $S_{11}$   $\Sigma$  resonances at 1630, 1675 and 1695 MeV [14]. The first one was associated with the two star  $\Sigma(1620)$  resonance, and the next one with the  $\Sigma(1750)$  resonance.

The  $\Sigma(1940)D_{13}$  resonance was not assigned in Table 13.4 of [13], whereas in [17] it was tentatively assigned as  ${}^48_{3/2}[70, 1^-]$ , the octet partner of  $N(1700)$ . In our calculation the lowest four  $D_{13}$   $\Sigma$  states are the spin-orbit partners of the  $S_{11}$  states at 1711, 1755, 1822 and 1974 MeV, the first one of which has been associated with the  $\Sigma(1670)$  resonance. We have assigned the  $\Sigma(1940)$  resonance as a member of the  $(v_1, v_2) = (0, 1)$  vibrational band with  ${}^28_{3/2}[56, 1^-]$  which occurs at 1974 MeV. This assignment is supported by its strong decay properties (see Sect. 6). In the relativized quark model there are three low-lying  $D_{13}$   $\Sigma$  states at 1655, 1750 and 1755 MeV [14], of which the first two were associated with the  $\Sigma(1670)$  and  $\Sigma(1940)$  resonances.

#### 4.2 Singlet resonances

There are three states which show a deviation of about 100 MeV or more from the data: the  $\Lambda^*(1405)$ ,  $\Lambda^*(1520)$  and  $\Lambda^*(2100)$  resonances are overpredicted by 236, 121 and 97 MeV, respectively. These three resonances are assigned as singlet states in Table IV (and were not included in the fitting procedure). An additional energy shift for the singlet states (without effecting the masses of the octet and decuplet states) can be obtained by adding to the mass formula of Eq. (4.1) a term that only acts on the singlet states

$$M^2 \rightarrow M^2 + \Delta M^2 \delta_{g_1,0} \delta_{g_2,0} . \quad (4.2)$$



This corresponds to a shift in the singlet masses of  $M\sqrt{1+(\Delta M^2/M^2)} \approx M[1+(\Delta M^2/2M^2)]$ . Since spin-orbit partners are shifted by the same amount, the mass splitting of 115 MeV between  $\Lambda^*(1405)$  and  $\Lambda^*(1520)$  cannot be reproduced by this mechanism. In principle, this splitting can be obtained from a spin-orbit interaction. However, in the rest of the baryon spectra there is no evidence for such a large spin-orbit coupling. This problem is common to  $qqq$  models of baryons (*e.g.* the constituent quark model with chromodynamics, either in its nonrelativistic [18] or its relativized form [14], and the chiral constituent quark model [19] all overpredict the  $\Lambda^*(1405)$  mass). Another explanation for the mass splitting between  $\Lambda^*(1520)$  and  $\Lambda^*(1405)$  is the proximity of the  $\Lambda^*(1405)$  resonance to the  $N\bar{K}$  threshold. The inclusion of the coupling to the  $N\bar{K}$  and  $\Sigma\pi$  decay channels produces a downward shift of the  $qqq$  state toward or even below the  $N\bar{K}$  threshold [20]. Such an interpretation is supported by the strong and electromagnetic couplings (see Sects. 6 and 8). In a chiral meson-baryon Lagrangian approach with an effective coupled-channel potential the  $\Lambda^*(1405)$  resonance emerges as a quasi-bound state of  $N\bar{K}$  [21].

### 4.3 Missing resonances

In Tables III and IV we presented the model states that could be associated with a three or four star resonance. In Tables V, VI and VII we show the masses of all low-lying octet, decuplet and singlet baryons. Since in the present approach no spin-orbit coupling has been taken into account, the states are grouped into multiplets labeled by  $L$ ,  $S$  and  $|L-S| \leq J \leq L+S$ . The multiplets for which at least one of its members has been associated with a three or four star resonance in Tables III or IV are labeled by  $\dagger$ . Tentative assignments of one or two star resonances are indicated by  $\ddagger$ . As in any  $qqq$  model of baryons there are many more calculated states than have been observed. The lowest so-called ‘missing’ resonances of the octet are associated with the  ${}^2\mathcal{8}_J[20, 1^+]$  state. Their calculated mass is given by 1713, 1849, 1826 and 1957 MeV for the  $N$ ,  $\Sigma$ ,  $\Lambda$  and  $\Xi$  resonances. The search for these ‘missing’ resonances is important in order to verify the assignments of the resonances and to distinguish between different models of baryons, such as three quark  $qqq$  vs. quark-diquark  $q-qq$  models which have less missing states because of the smaller number of degrees of freedom.

In a recent three-channel multi-resonance amplitude analysis by the Zagreb group [22] evidence was found for the existence of a third low-lying  $P_{11}$  state at  $1740 \pm 11$  MeV. The first two  $P_{11}$  states at  $1439 \pm 19$  MeV and  $1729 \pm 16$  MeV correspond to the  $N(1440)$  and  $N(1710)$  resonances of the PDG [13]. These  $P_{11}$  states were associated with the states at 1540, 1770 and 1880 MeV in the relativized quark model [23]. In the present calculation, they occur at 1444, 1683 and 1713 MeV, in good agreement with the analysis of the Zagreb group.

A recent analysis of new data on kaon photoproduction [24] has shown evidence for a  $D_{13}$  resonance at 1895 MeV [25]. In the present calculation, there are several possible assignments (see Table V). The lowest state that can be assigned to this new resonance is a vibrational excitation  $(v_1, v_2) = (0, 1)$  with  ${}^2\mathcal{8}_{3/2}[56, 1^-]$  and mass 1847 MeV. This state belongs to the same vibrational band as the  $N(1710)$  resonance, and is the octet partner of  $\Sigma(1940)$ . Another possible assignment is as a member of the ground state band  $(v_1, v_2) = (0, 0)$  with  ${}^2\mathcal{8}_{3/2}[70, 2^-]$  and mass 1874 MeV. However, this state is completely decoupled in strong and electromagnetic decays. Finally, there is a state that belongs to the same vibrational band  $(v_1, v_2) = (1, 0)$  as the  $N(1440)$  Roper resonance with  ${}^2\mathcal{8}_{3/2}[70, 1^-]$  and mass 1909 MeV. As far as the mass is concerned all three assignments are possible. The strong couplings for these states

provide a more sensitive tool to determine the most likely assignment (see Sect. 6). In the relativized quark model a  $D_{13}$  state has been predicted at 1960 MeV [14].

## 5 Strong couplings

Strong couplings provide an important test of baryon wave functions, and can be used to distinguish between different models of baryon structure. Here we consider strong decays of baryons by the emission of a pseudoscalar meson

$$B \rightarrow B' + M . \quad (5.1)$$

Several forms have been suggested for the form of the operator inducing the strong transition [26]. We use here the simple form [27]

$$\mathcal{H}_s = \frac{1}{(2\pi)^{3/2}(2k_0)^{1/2}} \sum_{j=1}^3 X_j^M \left[ 2g (\vec{s}_j \cdot \vec{k}) e^{-i\vec{k} \cdot \vec{r}_j} + h \vec{s}_j \cdot (\vec{p}_j e^{-i\vec{k} \cdot \vec{r}_j} + e^{-i\vec{k} \cdot \vec{r}_j} \vec{p}_j) \right] , \quad (5.2)$$

where  $\vec{r}_j$ ,  $\vec{p}_j$  and  $\vec{s}_j$  are the coordinate, momentum and spin of the  $j$ -th constituent, respectively;  $k_0$  is the meson energy and  $\vec{k} = k\hat{z}$  denotes the momentum carried by the outgoing meson. The coefficients  $g$  and  $h$  denote the strength of the two terms in the transition operator of Eq. (5.2). The flavor operator  $X_j^M$  corresponds to the emission of an elementary meson by the  $j$ -th constituent:  $q_j \rightarrow q'_j + M$  (see Figure 7).

Using the symmetry of the wave functions, transforming to Jacobi coordinates, integrating over the baryon center of mass coordinate, and adopting the rest frame of the initial baryon, the operator of Eq. (5.2) reduces to [5]

$$\mathcal{H}_s = \frac{1}{(2\pi)^{3/2}(2k_0)^{1/2}} 6X_3^M \left[ \left( gk - \frac{1}{6}hk \right) s_{3,z} \hat{U} - h s_{3,z} \hat{T}_z - \frac{1}{2}h (s_{3,+} \hat{T}_- + s_{3,-} \hat{T}_+) \right] , \quad (5.3)$$

with

$$\begin{aligned} \hat{U} &= e^{ik\sqrt{\frac{2}{3}}\lambda_z} , \\ \hat{T}_m &= \frac{1}{2} \left( \sqrt{\frac{2}{3}} p_{\lambda,m} e^{ik\sqrt{\frac{2}{3}}\lambda_z} + e^{ik\sqrt{\frac{2}{3}}\lambda_z} \sqrt{\frac{2}{3}} p_{\lambda,m} \right) . \end{aligned} \quad (5.4)$$

The calculation of the matrix elements of  $\mathcal{H}_s$  can be done in configuration space  $(\vec{\rho}, \vec{\lambda})$  or in momentum space  $(\vec{p}_\rho, \vec{p}_\lambda)$ . The mapping onto the algebraic space of  $U(7)$  is a convenient way to carry out the calculations, much in the same way as the mapping of coordinates and momenta onto creation and annihilation operators in the harmonic oscillator space. The operators  $\hat{U}$  and  $\hat{T}_m$  can be expressed algebraically by first making the replacement  $\vec{p}_\lambda/m_3 \rightarrow -ik_0\vec{\lambda}$  [28] and then mapping the coordinates onto the algebraic operators,  $\sqrt{2/3}\lambda_m \rightarrow \beta \hat{D}_{\lambda,m}/X_D$  [3, 4, 5]. The result is

$$\begin{aligned} \hat{U} &= e^{ik\beta \hat{D}_{\lambda,z}/X_D} , \\ \hat{T}_m &= -\frac{im_3 k_0 \beta}{2X_D} \left( \hat{D}_{\lambda,m} e^{ik\beta \hat{D}_{\lambda,z}/X_D} + e^{ik\beta \hat{D}_{\lambda,z}/X_D} \hat{D}_{\lambda,m} \right) . \end{aligned} \quad (5.5)$$

The dipole operator  $\hat{D}_{\lambda,m}$  is a generator of  $U(7)$  and  $X_D$  is its normalization, as discussed in [3, 4]. The spatial matrix elements of  $\hat{U}$  and  $\hat{T}_m$  are obtained in the collective model of baryons by folding with a

distribution function  $g(\beta)$  of charge and magnetization over the entire volume

$$g(\beta) = \beta^2 e^{-\beta/a} / 2a^3 . \quad (5.6)$$

All spatial matrix elements can be expressed in terms of the collective form factors

$$\begin{aligned} \mathcal{F}(k) &= \int d\beta g(\beta) \langle \psi' | \hat{U} | \psi \rangle , \\ \mathcal{G}_m(k) &= \int d\beta g(\beta) \langle \psi' | \hat{T}_m | \psi \rangle . \end{aligned} \quad (5.7)$$

Here  $|\psi\rangle$  and  $|\psi'\rangle$  denote the spatial wave functions of the initial and final baryons.

For strong decays in which the initial baryon  $B$  has angular momentum  $\vec{J} = \vec{L} + \vec{S}$  and in which the final baryon  $B'$  has  $L' = 0$  and thus  $J' = S'$ , the helicity amplitudes in the collective model are then given by

$$A_\nu(k) = \int d\beta g(\beta) \langle \Psi'(0, S', S', \nu) | \mathcal{H}_s | \Psi(L, S, J, \nu) \rangle , \quad (5.8)$$

Here  $|\Psi(L, S, J, M_J)\rangle$  and  $|\Psi'(0, S', S', \nu)\rangle$  denote the (space-spin-flavor) angular momentum coupled wave functions of the initial and final baryons, respectively (see Appendix B). The final baryon is a ground state baryon belonging either to the octet  ${}^2 8_{1/2}[56, 0^+]_{(0,0);0}$  or the decuplet  ${}^4 10_{3/2}[56, 0^+]_{(0,0);0}$ . The helicity amplitudes can be expressed in terms of a spatial matrix element and a spin-flavor matrix element

$$\begin{aligned} A_\nu(k) &= \frac{1}{(2\pi)^{3/2} (2k_0)^{1/2}} \left[ \langle L, 0, S, \nu | J, \nu \rangle \zeta_0 Z_0(k) + \frac{1}{2} \langle L, 1, S, \nu - 1 | J, \nu \rangle \zeta_+ Z_-(k) \right. \\ &\quad \left. + \frac{1}{2} \langle L, -1, S, \nu + 1 | J, \nu \rangle \zeta_- Z_+(k) \right] , \end{aligned} \quad (5.9)$$

with

$$\begin{aligned} Z_0(k) &= 6 \left( gk - \frac{1}{6} hk \right) \mathcal{F}(k) - 6h \mathcal{G}_z(k) , \\ Z_\pm(k) &= -6h \mathcal{G}_\pm(k) . \end{aligned} \quad (5.10)$$

In Table VIII we present the collective form factor  $\mathcal{F}(k)$  (for details of the derivation we refer to [3]). The form factors  $\mathcal{G}_m(k)$  are given by

$$\begin{aligned} \mathcal{G}_z(k) &= -\delta_{M,0} m_3 k_0 a \frac{d\mathcal{F}(k)}{dka} , \\ \mathcal{G}_\pm(k) &= \mp \delta_{M,\pm 1} m_3 k_0 a \sqrt{L(L+1)} \frac{\mathcal{F}(k)}{ka} . \end{aligned} \quad (5.11)$$

For any other model of baryons with the same spin-flavor structure, the corresponding results can be obtained by replacing Table VIII with the appropriate table (for example, by using harmonic oscillator wave functions as discussed in [3]).

The coefficients  $\zeta_m$  are the spin-flavor matrix elements of  $X_3^M s_{3,m}$  which can either be evaluated for each channel separately, or more conveniently, by using the Wigner-Eckart theorem and isoscalar factors of  $SU_f(3)$  [8]. The flavor wave functions are labeled by the quantum numbers  $(p, q)$ ,  $I, Y$  corresponding to the reduction  $SU_f(3) \supset SU_I(2) \otimes U_Y(1)$ . In this notation  $(p, q) = (g_1 - g_2, g_2)$ , and hence we have  $(p, q) = (1, 1)$ ,

(3, 0) or (0, 0) for the baryon flavor octet, decuplet and singlet, respectively, and  $(p, q) = (1, 1)$  or  $(0, 0)$  for the meson flavor octet and singlet, respectively. The spin-flavor matrix elements  $\zeta_m$  for a given isospin channel can be expressed as

$$\zeta_m = \sum_{\gamma} \left\langle \begin{array}{cc} (p_f, q_f) & (p, q) \\ I_f, Y_f & I, Y \end{array} \middle| \begin{array}{c} (p_i, q_i)_{\gamma} \\ I_i, Y_i \end{array} \right\rangle \alpha_{m, \gamma}. \quad (5.12)$$

The sum over  $\gamma$  is over different multiplicities. The  $SU(3)$  isoscalar factor which appears in Eq. (5.12) depends on the flavor multiplets  $(p, q)$ , the isospin  $I$  and the hypercharge  $Y$ . A compilation of the  $SU(3)$  isoscalar factors relevant for strong decays of baryons can be found in [13]. Results for a specific charge channel can be obtained by multiplying  $\zeta_m$  with the appropriate isospin Clebsch-Gordan coefficient  $\langle I_f, M_{I_f}, I, M_I | I_i, M_{I_i} \rangle$ .

In Tables IX–XII we present the coefficients  $\alpha_{m, \gamma}$  for strong decays into octet or decuplet baryons emitting a pseudoscalar meson (either octet or singlet). For strong decays of nonstrange baryons into the  $N\pi$ ,  $N\eta$ ,  $\Delta\pi$  and  $\Delta\eta$  channels the coefficients  $\zeta_m$  are given explicitly in Tables III and IV of [5]. Inspection of Tables IX–XII and the isoscalar factors on page 184 of [13] yields some interesting selection rules: (i) the  $B_{10} \rightarrow B_{10} + M_8$  decay

$$\Sigma^* \rightarrow \Sigma^* + \eta_8, \quad (5.13)$$

is forbidden since the  $SU(3)$  isoscalar factor vanishes, and (ii) there is a spin-flavor selection rule for the  ${}^4_8[70, L^P] \rightarrow {}^2_8[56, 0^+] + M_8$  decays

$$\begin{aligned} N &\rightarrow \Lambda + K, \\ \Lambda &\rightarrow N + \bar{K}, \\ \Xi &\rightarrow \Xi + \eta_8, \end{aligned} \quad (5.14)$$

which is similar to the Moorhouse selection rule in electromagnetic couplings [29]. However, the octet  $\eta_8$  and singlet  $\eta_1$  may mix because of  $SU_f(3)$  flavor symmetry breaking. The physical mesons  $\eta$  and  $\eta'$  are then given in terms of a mixing angle

$$\begin{aligned} \eta &= \eta_8 \cos \theta_P - \eta_1 \sin \theta_P, \\ \eta' &= \eta_8 \sin \theta_P + \eta_1 \cos \theta_P. \end{aligned} \quad (5.15)$$

The above mentioned forbidden two-body decays into a baryon and the octet meson  $\eta_8$ , are allowed for the physical mesons  $\eta$  and  $\eta'$  via the octet-singlet mixing.

## 6 Comparison with experimental strong decays

With the definition of the transition operator in Eq. (5.2) and the helicity amplitudes, the decay widths for a specific isospin channel are given by [26]

$$\Gamma(B \rightarrow B' + M) = 2\pi\rho \frac{2}{2J+1} \sum_{\nu>0} |A_{\nu}(k)|^2. \quad (6.1)$$

Here we adopt the procedure of [26], in which the decay widths are calculated in the rest frame of the decaying resonance, and in which the relativistic expression for the phase space factor  $\rho$  as well as for the momentum  $k$  of the emitted meson are retained. The expressions for  $k$  and  $\rho$  are

$$\begin{aligned} k^2 &= -m_M^2 + \frac{(m_B^2 - m_{B'}^2 + m_M^2)^2}{4m_B^2}, \\ \rho &= 4\pi \frac{E_{B'} E_M k}{m_B} \end{aligned} \quad (6.2)$$

with  $E_{B'} = \sqrt{m_{B'}^2 + k^2}$  and  $E_M = \sqrt{m_M^2 + k^2}$ . We consider here the strong decays of baryons in which a pseudoscalar meson (either octet or singlet) is emitted. The present calculation is an extension of [5] in which we only discussed nonstrange decays of nonstrange baryons.

The calculated widths depend on the two parameters  $g$  and  $h$  in the transition operator of Eq. (5.3), and on the scale parameter  $a$  of Eq. (5.6). In accordance with [5] we keep  $g$ ,  $h$  and  $a$  fixed for *all* resonances and *all* decay channels with the values  $g = 1.164$  fm,  $h = -0.094$  fm and  $a = 0.232$  fm (we note here that in [5] the values of  $g$  and  $h$  were given in  $\text{GeV}^{-1}$  instead of in fm). The decay widths of resonances that have been interpreted as a vibrational excitation of the string configuration of Fig. 1 depend on the coefficient  $\chi_1$  for  $(v_1, v_2) = (1, 0)$  (the  $N(1440)$ ,  $\Delta(1600)$ ,  $\Sigma(1660)$  and  $\Lambda(1600)$  resonances), or  $\chi_2$  for  $(v_1, v_2) = (0, 1)$  (the  $N(1710)$ ,  $\Sigma(1940)$  and  $\Lambda(1810)$  resonances) (see Table VIII). These coefficients are proportional to the intrinsic matrix element for each type of vibration. Here they are taken as constants with the values  $\chi_1 = 1.0$  [30] and  $\chi_2 = 0.7$ . For the pseudoscalar  $\eta$  mesons we introduce a mixing angle  $\theta_P = -23^\circ$  between the octet and singlet mesons [13]. This value is consistent with that determined in a study of meson spectroscopy [2].

In comparison with other studies, we note that in the calculation in the nonrelativistic quark model of [27] an elementary emission model is used, just as in the present calculation, but with the difference that the decay widths are parametrized by four reduced partial wave amplitudes instead of the two elementary amplitudes  $g$  and  $h$ . Furthermore, the momentum dependence of these reduced amplitudes is represented by a constant. The calculations in the relativized quark model are done in a pair-creation model for the decay and involve a different assumption on the phase space factor [31]. Both the nonrelativistic and relativized quark model calculations include the effects of mixing induced by the hyperfine interaction, which in the present calculations are not taken into account. It is important to note that we present a comparison of decay widths, rather than of decay amplitudes as was done in [27] and [31] for the nonrelativistic and relativized quark models.

In Tables XIII–XVII we compare the experimental strong decay widths of three and four star baryon resonances from the most recent compilation by the Particle Data Group [13] with the results of our calculation for the nucleon,  $\Delta$ ,  $\Sigma$ ,  $\Lambda$  and  $\Xi$  families. We have used the experimental value of the mass of the decaying baryon. Strong couplings of missing resonances belonging to the flavor octet, decuplet and singlet are presented in Tables XVIII–XXI, XXII–XXV and XXVI, respectively.

The calculated decay widths are to a large extent a consequence of spin-flavor symmetry and phase space. The use of the collective form factors of Table VIII introduces a power-law dependence on the meson momentum  $k$ , compared to, for example, an exponential dependence for harmonic oscillator form factors. Our results for the strong decay widths are in fair overall agreement with the available data, and show that the combination of a collective string-like  $qqq$  model of baryons and a simple elementary emission model for the decays can account for the main features of the data. There are a few exceptions

which could indicate evidence for the importance of degrees of freedom which are outside the present  $qqq$  model of baryons.

## 6.1 Nucleon resonances

The  $\pi$  and  $\eta$  decays of nucleon resonances have already been discussed in [5]. Whereas the  $\pi$  decays are in fair agreement with the data, the  $\eta$  decays of octet baryons show an unusual pattern: the  $S$ -wave states  $N(1535)$ ,  $\Sigma(1750)$  and  $\Lambda(1670)$  all are found experimentally to have a large branching ratio to the  $\eta$  channel, whereas the corresponding phase space factor is very small [15]. The small calculated  $\eta$  widths ( $< 0.5$  MeV) for these resonances are due to a combination of spin-flavor symmetry and the size of the phase space factor. The results of our analysis suggest that the observed  $\eta$  widths are not due to a conventional  $qqq$  state, but may rather indicate evidence for the presence of a state in the same mass region of a more exotic nature, such as a pentaquark configuration  $qqqq\bar{q}$  or a quasi-molecular  $S$ -wave resonance  $qqq\text{-}q\bar{q}$  just below or above threshold, bound by Van der Waals type forces (for example  $N\eta$ ,  $\Sigma K$  or  $\Lambda K$  [21]). In order to answer this question one has to carry out an analysis, similar to the present one, of the other configurations.

The  $K$  decays are suppressed with respect to the  $\pi$  decays because of phase space. In addition, the decay of the  $N(1650)$ ,  $N(1675)$  and  $N(1700)$  resonances into  $\Lambda K$  is forbidden by the spin-flavor selection rule for the decay of  ${}^4S[70, L^P]$  nucleon states into this channel (see Sect. 5). For  $N(1675)$  and  $N(1700)$  only an upper limit is known, whereas the  $N(1650)$  resonance has an observed width of  $12 \pm 7$  MeV. However, this resonance is just above the  $\Lambda K$  threshold which may lead to a coupling to a quasi-bound meson-baryon  $S$  wave resonance. A study of the effect of spin-flavor symmetry breaking on these decays is in progress.

## 6.2 Delta resonances

The strong decay widths of the  $\Delta$  resonances are in very good agreement with the available experimental data. The same holds for the other resonances that have been assigned as decuplet baryons:  $\Sigma^*(1385)$ ,  $\Sigma^*(2030)$  and  $\Xi^*(1530)$ . For the decuplet baryons there is no  $S$  state around the threshold of the various decay channels, so therefore there cannot be any coupling to quasi-molecular configurations. Just as for the nucleon resonances, the  $\eta$  and  $K$  decays are suppressed by phase space factors.

## 6.3 Sigma resonances

Strange resonances decay predominantly into the  $\pi$  and  $\bar{K}$  channel. Phase space factors suppress the  $\eta$  and  $K$  decays. The main discrepancy is found for  $\Sigma(1750)$ . In the discussion of nucleon resonances it was suggested that the  $S$  wave state  $\Sigma(1750)$  is the octet partner of  $N(1535)$ . It has a large observed  $\eta$  width despite the fact that there is hardly any phase space available for this decay. This may indicate that it has a large quasi-molecular component.

The assignment of  $\Sigma(1940)D_{13}$  as a member of the  $(v_1, v_2) = (0, 1)$  vibrational band with  ${}^2S_{3/2}[56, 1^-]$  and mass 1974 MeV is based on both its mass and its strong decay properties. If calculated with the observed mass, the other possible states,  ${}^2D_{3/2}[70, 1^-]$  and  ${}^4S_{3/2}[70, 1^-]$ , both have very large widths ( $\sim 100$  MeV) in the  $\Delta\bar{K}$  and  $\Sigma^*\pi$  channels, which is not supported by the data.

## 6.4 Lambda resonances

Also for  $\Lambda$  resonances the  $\eta$  and  $K$  decays are suppressed with respect to the  $\pi$  and  $\bar{K}$  channels because of phase space factors. Table XVI shows that the strong decays of  $\Lambda$  resonances show more discrepancies with the data than the other families of resonances.

We have assigned  $\Lambda(1670)$  as the octet partner of  $N(1535)$  and  $\Sigma(1750)$ . Its decay properties into the  $\eta$  channel have already been discussed in Sect. 6.1 on the nucleon resonances.

The spin-flavor selection rule that was discussed in Sect. 5 forbids the decay of  ${}^48[70, L^P]$   $\Lambda$  states into the  $N\bar{K}$  channel. Therefore, the calculated  $N\bar{K}$  widths of  $\Lambda(1800)$ ,  $\Lambda(1830)$  and  $\Lambda(2110)$  vanish, whereas all of them have been observed experimentally [13]. The  $\Lambda(1800)S_{01}$  state has large decay width into  $N\bar{K}^*(892)$  [13]. Since the mass of the resonance is just around the threshold of this channel, this could indicate a coupling with a quasi-molecular  $S$  wave. The  $N\bar{K}$  width of  $\Lambda(1830)$  is relatively small ( $6 \pm 3$  MeV), and hence in qualitative agreement with the selection rule. The situation for the  $\Lambda(2110)$  resonance is unclear.

The  $\Lambda^*(1405)$  resonance has a anomalously large decay width ( $50 \pm 2$  MeV) into  $\Sigma\pi$ . This feature emphasizes the quasi-molecular nature of  $\Lambda^*(1405)S_{01}$  due to the proximity of the  $N\bar{K}$  threshold. It has been shown [20] that the inclusion of the coupling to the  $N\bar{K}$  and  $\Sigma\pi$  decay channels produces a downward shift of the  $qqq$  state toward or even below the  $N\bar{K}$  threshold. In a chiral meson-baryon Lagrangian approach with an effective coupled-channel potential the  $\Lambda^*(1405)$  resonance emerges as a quasi-bound state of  $N\bar{K}$  [21].

## 6.5 Xi resonances

There is little experimental information available for the strong decays of baryons with strangeness  $-2$  ( $\Xi$ ) and  $-3$  ( $\Omega$ ). We find good agreement with the observed decay widths of the  $\Xi(1820)$  (octet) and the  $\Xi(1530)$  (decuplet) resonances (see Table XVII).

## 6.6 Missing resonances

For possible use in the analysis of new experimental data and in the search for missing resonances, we present in Tables XVIII–XXVI the strong decay widths of the missing resonances of Tables V–VII. The states with  $L^P = 1^+$ ,  $L^P = 2^-$  and  $[20, L^P]$  are decoupled because of spin-flavor symmetry. Most of the strong couplings of the low-lying missing resonances are small, which to a large extent explains their status [32]. Generally speaking, the orbital configurations that have the smallest strong couplings both for the octet, decuplet and singlet resonances are  $[56, 2^+]$  ( $v_1, v_2$ ) = (0, 0),  $[70, 1^-](1, 0)$  and  $[70, 1^-](0, 1)$ . It is interesting to note that in all cases the resonances associated with the configuration  $[56, 1^-](0, 1)$  exhibit large decay widths. The only resonance that we have assigned as one of these is  $\Sigma(1940)$ . The majority of the missing resonances with sizeable decay widths belong either to the configuration  $[56, 1^-](0, 1)$  or to  $[70, 2^+](0, 0)$ .

Tables XVIII and XXII show that the missing nucleon and  $\Delta$  resonances that are associated with the configurations  $[70, 2^+](0, 0)$ ,  $[70, 0^+](0, 1)$  and  $[56, 1^-](0, 1)$  are predicted to have a large decay width into the  $\pi$  channel. The  $\eta$  and  $K$  decays are suppressed with respect to the  $\pi$  decays because of phase space. Strange baryons decay predominantly into the  $\pi$  and  $\bar{K}$  channels. The  $\eta$  and  $K$  widths are

small in comparison, due to the available phase space. Inspection of Tables XIX–XXI shows that the dominant decay channels of the missing octet baryons are  $N\bar{K}$ ,  $\Sigma\pi$ ,  $\Delta\bar{K}$  for  $\Sigma$  resonances,  $N\bar{K}$ ,  $\Sigma^*\pi$  for  $\Lambda$  resonances, and  $\Sigma\bar{K}$ ,  $\Xi\pi$  for  $\Xi$  resonances. Similarly, we see from Tables XXIII–XXV that the missing decuplet baryons are most likely to couple to  $\Lambda\pi$ ,  $\Sigma^*\pi$  for  $\Sigma^*$  resonances, to  $\Sigma\bar{K}$ ,  $\Lambda\bar{K}$ ,  $\Xi\pi$ ,  $\Sigma^*\bar{K}$  for  $\Xi^*$  resonances, and to  $\Xi\bar{K}$  for  $\Omega$  resonances. Finally, Table XXVI shows that missing singlet baryons are most likely to decay into  $\Lambda^* \rightarrow N\bar{K}$ ,  $\Sigma\pi$ .

## 7 Electromagnetic couplings

In constituent models, electromagnetic couplings arise from the coupling of the (point-like) constituent parts to the electromagnetic field [33]. We discuss here the case of the emission of a lefthanded photon

$$B \rightarrow B' + \gamma, \quad (7.1)$$

for which the nonrelativistic part of the transverse electromagnetic coupling is given by

$$\mathcal{H}_{em} = 2\sqrt{\frac{\pi}{k_0}} \sum_{j=1}^3 \mu_j e_j \left[ k s_{j,-} e^{-i\vec{k}\cdot\vec{r}_j} + \frac{1}{2g_j} (p_{j,-} e^{-i\vec{k}\cdot\vec{r}_j} + e^{-i\vec{k}\cdot\vec{r}_j} p_{j,-}) \right], \quad (7.2)$$

where  $\vec{r}_j$ ,  $\vec{p}_j$  and  $\vec{s}_j$  are the coordinate, momentum and spin of the  $j$ -th constituent, respectively;  $k_0$  is the photon energy, and  $\vec{k} = k\hat{z}$  denotes the momentum carried by the outgoing photon. The photon is emitted by the  $j$ -th constituent:  $q_j \rightarrow q'_j + \gamma$  (see Figure 8). The transition operator can be simplified by using the symmetry of the baryon wave functions, transforming to Jacobi coordinates and integrating over the baryon center-of-mass coordinate, to obtain

$$\mathcal{H}_{em} = 6\sqrt{\frac{\pi}{k_0}} \mu_3 e_3 \left[ k s_{3,-} \hat{U} - \frac{1}{g_3} \hat{T}_- \right]. \quad (7.3)$$

The operators  $\hat{U}$  and  $\hat{T}_-$  are given in Eq. (5.5).

The transverse helicity amplitudes between the final ground state baryon belonging either to the  $J^P = 1/2^+$  octet with  ${}^2\mathcal{8}_{1/2}[56, 0^+]_{(0,0);0}$  or to the  $J^P = 3/2^+$  decuplet with  ${}^4\mathcal{10}_{3/2}[56, 0^+]_{(0,0);0}$ , and the initial (excited) state of a baryon resonance are expressed as [3]

$$\begin{aligned} \mathcal{A}_\nu(k) &= \int d\beta g(\beta) \langle \Psi'(0, S', S', \nu - 1) | \mathcal{H}_{em} | \Psi(L, S, J, \nu) \rangle, \\ &= 6\sqrt{\frac{\pi}{k_0}} \left[ k \langle L, 0; S, \nu | J, \nu \rangle \mathcal{B}_\nu - \langle L, 1; S, \nu - 1 | J, \nu \rangle \mathcal{A}_\nu \right], \end{aligned} \quad (7.4)$$

where  $\nu = 1/2, 3/2$  indicates the helicity. The orbit- and spin-flip amplitudes ( $\mathcal{A}_\nu$  and  $\mathcal{B}_\nu$ , respectively) are given by

$$\begin{aligned} \mathcal{B}_\nu &= \int d\beta g(\beta) \langle \Psi'(0, 0; S', \nu - 1) | \mu_3 e_3 s_{3,-} \hat{U} | \Psi(L, 0; S, \nu) \rangle, \\ \mathcal{A}_\nu &= \int d\beta g(\beta) \langle \Psi'(0, 0; S', \nu - 1) | \mu_3 e_3 \hat{T}_- / g_3 | \Psi(L, 1; S, \nu - 1) \rangle. \end{aligned} \quad (7.5)$$

Here  $|\Psi(L, M_L; S, M_S)\rangle$  denote the (space-spin-flavor) angular momentum uncoupled wave functions of the initial and final baryons (see Appendix B).



In Tables XXVII and XXVIII we show the orbit- and spin-flip amplitudes for some radiative hyperon decays. These results were obtained under the assumption of  $SU_f(3)$  flavor symmetry, *i.e.*  $\mu_3 = \mu_p$  and  $g_3 = g$ . The following selection rules apply: (i) the  ${}^4 10[56] \rightarrow {}^2 8[56] + \gamma$  decays

$$\begin{aligned}\Sigma^{*, -} &\rightarrow \Sigma^- + \gamma, \\ \Xi^{*, -} &\rightarrow \Xi^- + \gamma,\end{aligned}\tag{7.6}$$

are forbidden by  $U$ -spin conservation [34]. These decays can only occur if flavor symmetry is broken ( $m_d \neq m_s$ ). Also the  ${}^2 1[70] \rightarrow {}^4 10[56] + \gamma$  decay

$$\Lambda^* \rightarrow \Sigma^{*, 0} + \gamma,\tag{7.7}$$

is forbidden by  $U$ -spin selection rules but, contrary to the previous cases, remains forbidden in the case of flavor symmetry breaking.

## 8 Comparison with experimental electromagnetic couplings

Radiative hyperon decay widths can be calculated from the helicity amplitudes as [26]

$$\Gamma(B \rightarrow B' + \gamma) = 2\pi\rho \frac{1}{(2\pi)^3} \frac{2}{2J+1} \sum_{\nu>0} |A_\nu(k)|^2.\tag{8.1}$$

Just as for the strong couplings, the electromagnetic decay widths are calculated assuming  $SU_{sf}(6)$  spin-flavor symmetry and using the rest frame of the decaying resonance

$$\begin{aligned}k &= \frac{m_B^2 - m_{B'}^2}{2m_B}, \\ \rho &= 4\pi \frac{E_{B'} k^2}{m_B}\end{aligned}\tag{8.2}$$

with  $E_{B'} = \sqrt{m_{B'}^2 + k^2}$ . The scale parameter  $a$  was determined in a simultaneous fit to the proton charge radius, the proton electric and magnetic form factors and the neutron magnetic form factor to be  $a = 0.232$  fm [4]. This is the same value as has been determined independently in a fit of the  $N\pi$  decay widths of nucleon and delta resonances [5]. For all cases we take the quark  $g$  factors  $g = 1$ . The quark scale magnetic moment is equal to the proton magnetic moment  $\mu_p$ , which corresponds to a constituent quark mass  $m = 0.336$  GeV.

Recently, the SELEX collaboration has measured the charge radius of the  $\Sigma^-$  hyperon. The preliminary value is  $\langle r^2 \rangle_{\Sigma^-} = 0.60 \pm 0.08 \pm 0.08$  fm<sup>2</sup> [35]. This value is in good agreement with our predicted value of  $\langle r^2 \rangle_{\Sigma^-} = \langle r^2 \rangle_p = 12a^2 = 0.65$  fm<sup>2</sup>.

The radiative decays between baryons with  $L = 0$  and  $L' = 0$  only involve the magnetic transitions. The corresponding widths can be expressed in terms of the transition magnetic moments  $\mu_{BB'}(k)$  via

$$\sum_{\nu>0} |A_\nu(k)|^2 = 4\pi k \mu_{BB'}^2(k).\tag{8.3}$$

In Table XXIX we show the transition moments for the  ${}^2 8[56] \rightarrow {}^2 8[56] + \gamma$  and  ${}^4 10[56] \rightarrow {}^2 8[56] + \gamma$  transitions. In the absence of the form factor (*i.e.*  $\mathcal{F}(k) = 1$ ), we recover the symmetry relations between

the decuplet to octet transitions [36, 34]. For the conventions used in Appendices A and B we obtain the relations

$$\begin{aligned}
\mu_{\Sigma^0\Lambda} &= \frac{1}{\sqrt{3}}\mu_p, \\
\mu_{\Delta^+p} &= \mu_{\Delta^0n} = -\mu_{\Sigma^{*+}\Sigma^+} = -2\mu_{\Sigma^{*0}\Sigma^0} \\
&= \frac{2}{\sqrt{3}}\mu_{\Sigma^{*0}\Lambda} = -\mu_{\Xi^{*0}\Xi^0} = \frac{2\sqrt{2}}{3}\mu_p, \\
\mu_{\Sigma^{*-}\Sigma^-} &= \mu_{\Xi^{*-}\Xi^-} = 0.
\end{aligned} \tag{8.4}$$

The numerical values are given in the third column of Table XXIX. A comparison with the last column shows the reduction of the transition magnetic moments due to the form factor  $\mathcal{F}(k) = 1/(1+k^2a^2)^2$ .

The experimental information on radiative decays of hyperons is very limited. In Table XXX we present the radiative decay widths of low-lying hyperon resonances, and compare wherever possible with the data. The  $\Delta^+ \rightarrow p + \gamma$  decay width is underpredicted by 35 %, a common feature of all  $qqq$  constituent quark models. This discrepancy has been shown to be due to nonresonant meson-exchange mechanisms [40]. Just as for the energies and the strong decays, the  $\Lambda^*(1405)$  resonance shows large deviations for the radiative decay widths, which once again confirms its uncertain nature as a  $qqq$  state. The forbidden decays  $\Lambda^*(1405) \rightarrow \Sigma^{*0} + \gamma$  and  $\Lambda^*(1520) \rightarrow \Sigma^{*0} + \gamma$  have not been observed. For comparison we also present the radiative decay widths of decuplet hyperons as obtained from lattice calculations [41] and from a chiral constituent quark model with electromagnetic exchange currents between quarks [42]. The negative parity hyperon decay widths for  $\Sigma^{*,-} \rightarrow \Sigma^- + \gamma$  and  $\Xi^{*,-} \rightarrow \Xi^- + \gamma$  have a small nonvanishing value in [41, 42], whereas in the present calculation they are forbidden by flavor symmetry selection rules. In a subsequent publication we plan to investigate the effects of  $SU_f(3)$  flavor symmetry breaking on the electromagnetic couplings.

## 9 Summary and conclusions

We have presented in this article a systematic analysis of spectra and transition rates of strange baryons in the framework of a collective string-like  $qqq$  model, in which the orbitally excited baryons are interpreted as collective rotations and vibrations of the strings. The algebraic structure of the model, both for the internal degrees of freedom of spin-flavor-color and for the spatial degrees of freedom, has been used to derive transparent results, such as a mass formula, selection rules and closed expressions for strong and electromagnetic couplings.

The situation is similar to that encountered for nonstrange baryons. While spectra are reasonably well described, transition rates, especially strong decay widths are only qualitatively described. The combination of a collective string-like  $qqq$  model of baryons and a simple elementary emission model for the decays can account for the main features of the data. The main discrepancies are found for the low-lying  $S$ -wave states, specifically  $N(1535)$ ,  $\Sigma(1750)$ ,  $\Lambda^*(1405)$ ,  $\Lambda(1670)$  and  $\Lambda(1800)$ . All of these resonances have masses which are close to the threshold of a meson-baryon decay channel, and hence they could mix with a quasi-molecular  $S$  wave resonance of the form  $qqq - q\bar{q}$ . In contrary, decuplet baryons have no low-lying  $S$  states with masses close to the threshold of a particular decay channel, and their spectroscopy is described very well. The results of our analysis suggest that in future experiments

particular attention be paid to the resonances mentioned above in order to elucidate their structure, and to look for evidence of the existence of exotic (non  $qqq$ ) configurations of quarks and gluons.

In our calculations we have included only a diagonal breaking of the spin-flavor symmetry. This seems to be a good approximation to the actual situation and no major discrepancy appear to be related to non-diagonal breakings. A study of the effects of  $SU_f(3)$  flavor symmetry breaking due to different quark masses on the radiative decays and strong couplings is in progress, and will be published separately.

This paper concludes our analysis of  $q^3$  configurations in baryons. The next step is the study of more complex configurations of quarks and gluons, such as hybrid quark-gluon states  $qqq-g$ , pentaquark states  $q^4\bar{q}$  and multiquark meson-baryon bound states  $qqq-q\bar{q}$ .

## Acknowledgements

This work is supported in part by DGAPA-UNAM under project IN101997, by CONACyT under project 32416-E and by D.O.E. Grant DE-FG02-91ER40608.

## A Spin-flavor wave functions

Here we list the conventions used for the spin and flavor wave functions which are consistent with the choice of Jacobi coordinates of Eq. (2.3). They coincide with the conventions of [27].

### A.1 Spin wave functions

The spin wave functions  $|S, M_S\rangle$  are given by [27]:

$$\begin{aligned}
|1/2, 1/2\rangle &: \chi_\rho = [|\uparrow\downarrow\uparrow\rangle - |\downarrow\uparrow\uparrow\rangle]/\sqrt{2}, \\
&: \chi_\lambda = [2|\uparrow\uparrow\downarrow\rangle - |\uparrow\downarrow\uparrow\rangle - |\downarrow\uparrow\uparrow\rangle]/\sqrt{6}, \\
|3/2, 3/2\rangle &: \chi_S = |\uparrow\uparrow\uparrow\rangle.
\end{aligned} \tag{A.1}$$

We only show the state with the largest component of the projection  $M_S = S$ . The other states are obtained by applying the lowering operator in spin space.

### A.2 Flavor wave functions

For the flavor wave functions  $|(p, q), I, M_I, Y\rangle$  we adopt the convention of [8] with  $(p, q) = (g_1 - g_2, g_2)$ .

(i) The octet baryons  $(p, q) = (1, 1)$ :

$$\begin{aligned}
|(1, 1), 1/2, 1/2, 1\rangle &: \phi_\rho(p) = [|\udu\rangle - |\duu\rangle]/\sqrt{2}, \\
&: \phi_\lambda(p) = [2|\uud\rangle - |\udu\rangle - |\duu\rangle]/\sqrt{6}, \\
|(1, 1), 1, 1, 0\rangle &: \phi_\rho(\Sigma^+) = [|\suu\rangle - |\usu\rangle]/\sqrt{2}, \\
&: \phi_\lambda(\Sigma^+) = [|\suu\rangle + |\usu\rangle - 2|\uus\rangle]/\sqrt{6}, \\
|(1, 1), 0, 0, 0\rangle &: \phi_\rho(\Lambda) = [2|\uds\rangle - 2|\dus\rangle - |\dsu\rangle + |\sdu\rangle - |\sud\rangle + |\usd\rangle]/\sqrt{12}, \\
&: \phi_\lambda(\Lambda) = [-|\dsu\rangle - |\sdu\rangle + |\sud\rangle + |\usd\rangle]/2,
\end{aligned}$$

$$\begin{aligned}
|(1, 1), 1/2, 1/2, -1\rangle &: \phi_\rho(\Xi^0) = [|sus\rangle - |uss\rangle]/\sqrt{2}, \\
&: \phi_\lambda(\Xi^0) = [2|ssu\rangle - |sus\rangle - |uss\rangle]/\sqrt{6}.
\end{aligned} \tag{A.2}$$

(ii) The decuplet baryons  $(p, q) = (3, 0)$ :

$$\begin{aligned}
|(3, 0), 3/2, 3/2, 1\rangle &: \phi_S(\Delta^{++}) = |uuu\rangle, \\
|(3, 0), 1, 1, 0\rangle &: \phi_S(\Sigma^+) = [|suu\rangle + |usu\rangle + |uus\rangle]/\sqrt{3}, \\
|(3, 0), 1/2, 1/2, -1\rangle &: \phi_S(\Xi^0) = [|ssu\rangle + |sus\rangle + |uss\rangle]/\sqrt{3}, \\
|(3, 0), 0, 0, -2\rangle &: \phi_S(\Omega^-) = |sss\rangle.
\end{aligned} \tag{A.3}$$

(iii) The singlet baryons  $(p, q) = (0, 0)$ :

$$|(0, 0), 0, 0, 0\rangle : \phi_A(\Lambda) = [|uds\rangle - |dus\rangle + |dsu\rangle - |sdu\rangle + |sud\rangle - |usd\rangle]/\sqrt{6}. \tag{A.4}$$

We only show the highest charge state  $M_I = I$  with  $Q = I + Y/2$ . The other charge states are obtained by applying the lowering operator in isospin space.

## B Baryon wave functions

The  $S_3$  invariant space-spin-flavor ( $\Psi = \psi\chi\phi$ ) baryon wave functions are given by

$$\begin{aligned}
{}^2_8[56, L^P] &: \psi_S(\chi_\rho\phi_\rho + \chi_\lambda\phi_\lambda)/\sqrt{2}, \\
{}^2_8[70, L^P] &: [\psi_\rho(\chi_\rho\phi_\lambda + \chi_\lambda\phi_\rho) + \psi_\lambda(\chi_\rho\phi_\rho - \chi_\lambda\phi_\lambda)]/2, \\
{}^4_8[70, L^P] &: (\psi_\rho\phi_\rho + \psi_\lambda\phi_\lambda)\chi_S/\sqrt{2}, \\
{}^2_8[20, L^P] &: \psi_A(\chi_\rho\phi_\lambda - \chi_\lambda\phi_\rho)/\sqrt{2}, \\
{}^4_{10}[56, L^P] &: \psi_S\chi_S\phi_S, \\
{}^2_{10}[70, L^P] &: (\psi_\rho\chi_\rho + \psi_\lambda\chi_\lambda)\phi_S/\sqrt{2}, \\
{}^2_1[70, L^P] &: (\psi_\rho\chi_\lambda - \psi_\lambda\chi_\rho)\phi_A/\sqrt{2}, \\
{}^4_1[20, L^P] &: \psi_A\chi_S\phi_A.
\end{aligned} \tag{B.1}$$

The quark orbital angular momentum  $L$  is coupled with the spin  $S$  to the total angular momentum  $J$  of the baryon.

## References

- [1] See *e.g.* ‘Proceedings of the 8th International Conference on the Structure of Baryons: Baryons 98’, Eds. D.W. Menze and B.Ch. Metsch, World Scientific, Singapore, 1999.
- [2] F. Iachello, N.C. Mukhopadhyay and L. Zhang, *Phys. Rev. D* **44** (1991), 898; F. Iachello and D. Kusnezov, *Phys. Rev. D* **45** (1992), 4156; C. Gobbi, F. Iachello and D. Kusnezov, *Phys. Rev. D* **50** (1994), 2048.
- [3] R. Bijker, F. Iachello and A. Leviatan, *Ann. Phys. (N.Y.)* **236** (1994), 69.
- [4] R. Bijker, F. Iachello and A. Leviatan, *Phys. Rev. C* **54** (1996), 1935.
- [5] R. Bijker, F. Iachello and A. Leviatan, *Phys. Rev. D* **55** (1997), 2862.
- [6] R. Bijker and A. Leviatan, *Few-Body Systems* **25** (1998), 89.
- [7] K.C. Bowler, P.J. Corvi, A.J.G. Hey, P.D. Jarvis and R.C. King, *Phys. Rev. D* **24** (1981), 197; A.J.G. Hey and R.L. Kelly, *Phys. Rep.* **96** (1983), 71.
- [8] J.J. de Swart, *Rev. Mod. Phys.* **35** (1963), 916.
- [9] P. Kramer and M. Moshinsky, *Nucl. Phys* **82** (1966), 241; M. Moshinsky and Yu.F. Smirnov, ‘The harmonic oscillator in modern physics: from atoms to quarks’, Gordon and Breach, 1996.
- [10] J.P. Elliott, *Proc. Roy. Soc. A* **245** (1958), 128 and 562.
- [11] F. Gürsey and L.A. Radicati, *Phys. Rev. Lett.* **13** (1964), 173.
- [12] F.J. Squires, *Nuovo Cimento* **25** (1962), 242; A. Martin, *Phys. Lett.* **1** (1962), 72.
- [13] Particle Data Group, *Eur. Phys. J. C* **3** (1998), 1.
- [14] S. Capstick and N. Isgur, *Phys. Rev. D* **34** (1986), 2809.
- [15] B.M.K. Nefkens, in ‘Proceedings of the Fourth CEBAF/INT Workshop:  $N^*$  Physics’, Eds. T.-S.H. Lee and W. Roberts, World Scientific, Singapore, 1997, p. 186.
- [16] F. Iachello, ‘Proceedings of the Fourth CEBAF/INT Workshop:  $N^*$  Physics’, Eds. T.-S.H. Lee and W. Roberts, World Scientific, Singapore, 1997, p. 78.
- [17] S. Gasiorowicz and J.L. Rosner, *Am. J. Phys.* **49** (1981), 954.
- [18] N. Isgur and G. Karl, *Phys. Rev. D* **18** (1978), 4187; *ibid.* **19** (1979), 2653; *ibid.* **20** (1979), 1191; K.-T. Chao, N. Isgur and G. Karl, *Phys. Rev. D* **23** (1981), 155.
- [19] L.Ya. Glozman, W. Plessas, K. Varga and R.F. Wagenbrunn, *Phys. Rev. D* **58** (1998), 094030.
- [20] M. Arima, S. Matsui and K. Shimizu, *Phys. Rev. C* **49** (1994), 2831.
- [21] N. Kaiser, T. Waas and W. Weise, *Nucl. Phys. A* **612** (1997), 297.

- [22] M. Batinić, I. Dadić, I. Šlaus, A. Švarc, B.M.K. Nefkens and T.-S.H. Lee, *Phys. Scr.* **58** (1998), 15.
- [23] S. Capstick, T.-S.H. Lee, W. Roberts and A. Švarc, *Phys. Rev. C* **59** (1999), R3002.
- [24] M.Q. Tran et al., *Phys. Lett. B* **445** (1998), 20.
- [25] T. Mart and C. Bennhold, *Phys. Rev. C* **61** (2000), 012201.
- [26] A. Le Yaouanc, L. Oliver, O. Pène and J.-C. Raynal, ‘Hadron transitions in the quark model’, Gordon and Breach (1988).
- [27] R. Koniuk and N. Isgur, *Phys. Rev. D* **21** (1980), 1868.
- [28] R. McClary and N. Byers, *Phys. Rev. D* **28** (1983), 1692.
- [29] R.G. Moorhouse, *Phys. Rev. Lett.* **16** (1966), 772.
- [30] E. Tomasi-Gustafsson, M.P. Rekalo, R. Bijker, A. Leviatan and F. Iachello, *Phys. Rev. C* **59** (1999), 1526.
- [31] S. Capstick and W. Roberts, *Phys. Rev. D* **47** (1993), 1994; *Phys. Rev. D* **49** (1994), 4570; *Phys. Rev. D* **58** (1998), 074011.
- [32] R. Koniuk and N. Isgur, *Phys. Rev. Lett.* **44** (1980), 845.
- [33] L.A. Copley, G. Karl and E. Obryk, *Phys. Lett. B* **29** (1969), 117; L.A. Copley, G. Karl and E. Obryk, *Nucl. Phys. B* **13** (1969), 303.
- [34] L.G. Landsberg, *Physics of Atomic Nuclei*, **59** (1996), 2080.
- [35] I. Eschrich, in ‘Baryons ’98, Proceedings of the 8th International Conference on the Structure of Baryons’, Eds. D.W. Menze and B.Ch. Metsch, World Scientific (1999), p. 450; B. Povh, preprint hep-ph/9908233.
- [36] M.A.B. Bég, B.W. Lee and A. Pais, *Phys. Rev. Lett.* **13** (1964), 514.
- [37] P.C. Peterson, A. Beretvas, T. Devlin, K.B. Luk, G.B. Thomson, R. Whitman, R. Handler, B. Lundberg, L. Pondrom, M. Sheaff, C. Wilkinson, P. Border, J. Dworkin, O.E. Overseth, R. Rameika, G. Valenti, K. Heller and C. James, *Phys. Rev. Lett.* **57** (1986), 949.
- [38] T.S. Mast, M. Alston-Garnjost, R.O. Bangerter, A. Barbaro-Galtieri, L.K. Gershwin, F.T. Solmitz and R.D. Tripp, *Phys. Rev. Lett.* **21** (1968), 1715.
- [39] R. Bertini, *Nucl. Phys. B* **279** (1987), 49.
- [40] T. Sato and T.-S.H. Lee, *Phys. Rev. C* **54** (1996), 2660.
- [41] D.B. Leinweber, T. Draper and R.M. Woloshyn, *Phys. Rev. D* **48** (1993), 2230.
- [42] G. Wagner, A.J. Buchmann and A. Faessler, *Phys. Rev. C* **58** (1998), 1745.

Table I: Classification of ground state baryons.

|                                 | Baryon      | I   | Y  |
|---------------------------------|-------------|-----|----|
| $J^P = \frac{1}{2}^+$ octet:    | $N$         | 1/2 | 1  |
|                                 | $\Sigma$    | 1   | 0  |
|                                 | $\Lambda$   | 0   | 0  |
|                                 | $\Xi$       | 1/2 | -1 |
| $J^P = \frac{3}{2}^+$ decuplet: | $\Delta$    | 3/2 | 1  |
|                                 | $\Sigma^*$  | 1   | 0  |
|                                 | $\Xi^*$     | 1/2 | -1 |
|                                 | $\Omega$    | 0   | -2 |
| $J^P = \frac{1}{2}^+$ singlet:  | $\Lambda^*$ | 0   | 0  |

Table II: Values of the parameters in the mass formula of Eq. (4.1) in  $\text{GeV}^2$ .

| Parameter            | Present | Ref. [3] |
|----------------------|---------|----------|
| $M_0^2$              | 0.882   | 0.882    |
| $\kappa_1$           | 1.204   | 1.192    |
| $\kappa_2$           | 1.460   | 1.535    |
| $\alpha$             | 1.068   | 1.064    |
| $a$                  | -0.041  | -0.042   |
| $b$                  | 0.017   | 0.030    |
| $c$                  | 0.130   | 0.124    |
| $d$                  | -0.449  |          |
| $e$                  | 0.016   |          |
| $f$                  | 0.042   |          |
| $\delta(\text{MeV})$ | 33      | 39       |



Table III: Mass spectrum of nonstrange baryon resonances in the oblate top model. The masses are given in MeV. The experimental values are taken from [13].

| Baryon $L_{2I,2J}$     | Status | Mass      | State                             | $(v_1, v_2)$ | $M_{\text{calc}}$ |
|------------------------|--------|-----------|-----------------------------------|--------------|-------------------|
| $N(939)P_{11}$         | ****   | 939       | ${}^2\mathbf{8}_{1/2}[56, 0^+]$   | (0,0)        | 939               |
| $N(1440)P_{11}$        | ****   | 1430-1470 | ${}^2\mathbf{8}_{1/2}[56, 0^+]$   | (1,0)        | 1444              |
| $N(1520)D_{13}$        | ****   | 1515-1530 | ${}^2\mathbf{8}_{3/2}[70, 1^-]$   | (0,0)        | 1563              |
| $N(1535)S_{11}$        | ****   | 1520-1555 | ${}^2\mathbf{8}_{1/2}[70, 1^-]$   | (0,0)        | 1563              |
| $N(1650)S_{11}$        | ****   | 1640-1680 | ${}^4\mathbf{8}_{1/2}[70, 1^-]$   | (0,0)        | 1683              |
| $N(1675)D_{15}$        | ****   | 1670-1685 | ${}^4\mathbf{8}_{5/2}[70, 1^-]$   | (0,0)        | 1683              |
| $N(1680)F_{15}$        | ****   | 1675-1690 | ${}^2\mathbf{8}_{5/2}[56, 2^+]$   | (0,0)        | 1737              |
| $N(1700)D_{13}$        | ***    | 1650-1750 | ${}^4\mathbf{8}_{3/2}[70, 1^-]$   | (0,0)        | 1683              |
| $N(1710)P_{11}$        | ***    | 1680-1740 | ${}^2\mathbf{8}_{1/2}[70, 0^+]$   | (0,1)        | 1683              |
| $N(1720)P_{13}$        | ****   | 1650-1750 | ${}^2\mathbf{8}_{3/2}[56, 2^+]$   | (0,0)        | 1737              |
| $N(2190)G_{17}$        | ****   | 2100-2200 | ${}^2\mathbf{8}_{7/2}[70, 3^-]$   | (0,0)        | 2140              |
| $N(2220)H_{19}$        | ****   | 2180-2310 | ${}^2\mathbf{8}_{9/2}[56, 4^+]$   | (0,0)        | 2271              |
| $N(2250)G_{19}$        | ****   | 2170-2310 | ${}^4\mathbf{8}_{9/2}[70, 3^-]$   | (0,0)        | 2229              |
| $N(2600)I_{1,11}$      | ***    | 2550-2750 | ${}^2\mathbf{8}_{11/2}[70, 5^-]$  | (0,0)        | 2591              |
| $\Delta(1232)P_{33}$   | ****   | 1230-1234 | ${}^4\mathbf{10}_{3/2}[56, 0^+]$  | (0,0)        | 1246              |
| $\Delta(1600)P_{33}$   | ***    | 1550-1700 | ${}^4\mathbf{10}_{3/2}[56, 0^+]$  | (1,0)        | 1660              |
| $\Delta(1620)S_{31}$   | ****   | 1615-1675 | ${}^2\mathbf{10}_{1/2}[70, 1^-]$  | (0,0)        | 1649              |
| $\Delta(1700)D_{33}$   | ****   | 1670-1770 | ${}^2\mathbf{10}_{3/2}[70, 1^-]$  | (0,0)        | 1649              |
| $\Delta(1905)F_{35}$   | ****   | 1870-1920 | ${}^4\mathbf{10}_{5/2}[56, 2^+]$  | (0,0)        | 1921              |
| $\Delta(1910)P_{31}$   | ****   | 1870-1920 | ${}^4\mathbf{10}_{1/2}[56, 2^+]$  | (0,0)        | 1921              |
| $\Delta(1920)P_{33}$   | ***    | 1900-1970 | ${}^4\mathbf{10}_{3/2}[56, 2^+]$  | (0,0)        | 1921              |
| $\Delta(1930)D_{35}$   | ***    | 1920-1970 | ${}^2\mathbf{10}_{5/2}[70, 2^-]$  | (0,0)        | 1946              |
| $\Delta(1950)F_{37}$   | ****   | 1940-1960 | ${}^4\mathbf{10}_{7/2}[56, 2^+]$  | (0,0)        | 1921              |
| $\Delta(2420)H_{3,11}$ | ****   | 2300-2500 | ${}^4\mathbf{10}_{11/2}[56, 4^+]$ | (0,0)        | 2414              |

Table IV: As Table III, but for strange baryon resonances. Note, that  $\Xi$  resonances are denoted by  $L_{2I,2J}$ .

| Baryon $L_{I,2J}$       | Status | Mass      | State                  | $(v_1, v_2)$ | $M_{\text{calc}}$ |
|-------------------------|--------|-----------|------------------------|--------------|-------------------|
| $\Sigma(1193)P_{11}$    | ****   | 1193      | $^2 8_{1/2}[56, 0^+]$  | (0,0)        | 1170              |
| $\Sigma(1660)P_{11}$    | ***    | 1630-1690 | $^2 8_{1/2}[56, 0^+]$  | (1,0)        | 1604              |
| $\Sigma(1670)D_{13}$    | ****   | 1665-1685 | $^2 8_{3/2}[70, 1^-]$  | (0,0)        | 1711              |
| $\Sigma(1750)S_{11}$    | ***    | 1730-1800 | $^2 8_{1/2}[70, 1^-]$  | (0,0)        | 1711              |
| $\Sigma(1775)D_{15}$    | ****   | 1770-1780 | $^4 8_{5/2}[70, 1^-]$  | (0,0)        | 1822              |
| $\Sigma(1915)F_{15}$    | ****   | 1900-1935 | $^2 8_{5/2}[56, 2^+]$  | (0,0)        | 1872              |
| $\Sigma(1940)D_{13}$    | ***    | 1900-1950 | $^2 8_{3/2}[56, 1^-]$  | (0,1)        | 1974              |
| $\Sigma^*(1385)P_{13}$  | ****   | 1383-1385 | $^4 10_{3/2}[56, 0^+]$ | (0,0)        | 1382              |
| $\Sigma^*(2030)F_{17}$  | ****   | 2025-2040 | $^4 10_{7/2}[56, 2^+]$ | (0,0)        | 2012              |
| $\Lambda(1116)P_{01}$   | ****   | 1116      | $^2 8_{1/2}[56, 0^+]$  | (0,0)        | 1133              |
| $\Lambda(1600)P_{01}$   | ***    | 1560-1700 | $^2 8_{1/2}[56, 0^+]$  | (1,0)        | 1577              |
| $\Lambda(1670)S_{01}$   | ****   | 1660-1680 | $^2 8_{1/2}[70, 1^-]$  | (0,0)        | 1686              |
| $\Lambda(1690)D_{03}$   | ****   | 1685-1690 | $^2 8_{3/2}[70, 1^-]$  | (0,0)        | 1686              |
| $\Lambda(1800)S_{01}$   | ***    | 1720-1850 | $^4 8_{1/2}[70, 1^-]$  | (0,0)        | 1799              |
| $\Lambda(1810)P_{01}$   | ***    | 1750-1850 | $^2 8_{1/2}[70, 0^+]$  | (0,1)        | 1799              |
| $\Lambda(1820)F_{05}$   | ****   | 1815-1825 | $^2 8_{5/2}[56, 2^+]$  | (0,0)        | 1849              |
| $\Lambda(1830)D_{05}$   | ****   | 1810-1830 | $^4 8_{5/2}[70, 1^-]$  | (0,0)        | 1799              |
| $\Lambda(1890)P_{03}$   | ****   | 1850-1910 | $^2 8_{3/2}[56, 2^+]$  | (0,0)        | 1849              |
| $\Lambda(2110)F_{05}$   | ****   | 2090-2140 | $^4 8_{5/2}[70, 2^+]$  | (0,0)        | 2074              |
| $\Lambda(2350)H_{09}$   | ***    | 2340-2370 | $^2 8_{9/2}[56, 4^+]$  | (0,0)        | 2357              |
| $\Lambda^*(1405)S_{01}$ | ****   | 1402-1410 | $^2 1_{1/2}[70, 1^-]$  | (0,0)        | 1641              |
| $\Lambda^*(1520)D_{03}$ | ****   | 1518-1520 | $^2 1_{3/2}[70, 1^-]$  | (0,0)        | 1641              |
| $\Lambda^*(2100)G_{07}$ | ****   | 2090-2110 | $^2 1_{7/2}[70, 3^-]$  | (0,0)        | 2197              |
| $\Xi(1318)P_{11}$       | ****   | 1314-1316 | $^2 8_{1/2}[56, 0^+]$  | (0,0)        | 1334              |
| $\Xi(1820)D_{13}$       | ***    | 1818-1828 | $^2 8_{3/2}[70, 1^-]$  | (0,0)        | 1828              |
| $\Xi^*(1530)P_{13}$     | ****   | 1531-1532 | $^4 10_{3/2}[56, 0^+]$ | (0,0)        | 1524              |
| $\Omega(1672)P_{03}$    | ****   | 1672-1673 | $^4 10_{3/2}[56, 0^+]$ | (0,0)        | 1670              |

Table V: Masses of low-lying octet baryons in MeV. Assignments of three and four star resonances are labeled by  $\dagger$ , and tentative assignments of one and two star resonances by  $\ddagger$ .

| State                       | $(v_1, v_2)$ | $N$             | $\Sigma$        | $\Lambda$      | $\Xi$          |
|-----------------------------|--------------|-----------------|-----------------|----------------|----------------|
| ${}^2\mathbf{8}_J[56, 0^+]$ | (0,0)        | 939 $\dagger$   | 1170 $\dagger$  | 1133 $\dagger$ | 1334 $\dagger$ |
| ${}^2\mathbf{8}_J[70, 1^-]$ | (0,0)        | 1563 $\dagger$  | 1711 $\dagger$  | 1686 $\dagger$ | 1828 $\dagger$ |
| ${}^4\mathbf{8}_J[70, 1^-]$ | (0,0)        | 1683 $\dagger$  | 1822 $\dagger$  | 1799 $\dagger$ | 1932           |
| ${}^2\mathbf{8}_J[20, 1^+]$ | (0,0)        | 1713            | 1849            | 1826           | 1957           |
| ${}^2\mathbf{8}_J[56, 2^+]$ | (0,0)        | 1737 $\dagger$  | 1872 $\dagger$  | 1849 $\dagger$ | 1979           |
| ${}^2\mathbf{8}_J[70, 2^+]$ | (0,0)        | 1874 $\ddagger$ | 1999            | 1978           | 2100           |
| ${}^2\mathbf{8}_J[70, 2^-]$ | (0,0)        | 1874            | 1999            | 1978           | 2100           |
| ${}^4\mathbf{8}_J[70, 2^+]$ | (0,0)        | 1975 $\ddagger$ | 2095            | 2074 $\dagger$ | 2191           |
| ${}^4\mathbf{8}_J[70, 2^-]$ | (0,0)        | 1975            | 2095            | 2074           | 2191           |
| ${}^2\mathbf{8}_J[56, 0^+]$ | (1,0)        | 1444 $\dagger$  | 1604 $\dagger$  | 1577 $\dagger$ | 1727           |
| ${}^2\mathbf{8}_J[70, 1^-]$ | (1,0)        | 1909            | 2033            | 2012           | 2132           |
| ${}^4\mathbf{8}_J[70, 1^-]$ | (1,0)        | 2009            | 2127            | 2107           | 2222           |
| ${}^2\mathbf{8}_J[20, 1^+]$ | (1,0)        | 2034            | 2150            | 2130           | 2244           |
| ${}^2\mathbf{8}_J[70, 0^+]$ | (0,1)        | 1683 $\dagger$  | 1822 $\ddagger$ | 1799 $\dagger$ | 1932           |
| ${}^4\mathbf{8}_J[70, 0^+]$ | (0,1)        | 1796            | 1926            | 1904           | 2030           |
| ${}^2\mathbf{8}_J[56, 1^-]$ | (0,1)        | 1847            | 1974 $\dagger$  | 1952           | 2076           |
| ${}^2\mathbf{8}_J[70, 1^-]$ | (0,1)        | 1975            | 2095            | 2074           | 2191           |
| ${}^2\mathbf{8}_J[70, 1^+]$ | (0,1)        | 1975            | 2095            | 2074           | 2191           |
| ${}^4\mathbf{8}_J[70, 1^-]$ | (0,1)        | 2072            | 2186            | 2167           | 2278           |
| ${}^4\mathbf{8}_J[70, 1^+]$ | (0,1)        | 2072            | 2186            | 2167           | 2278           |
| ${}^2\mathbf{8}_J[20, 1^-]$ | (0,1)        | 2096            | 2209            | 2190           | 2300           |

Table VI: As Table V, but for decuplet baryons.

| State                | $(v_1, v_2)$ | $\Delta$          | $\Sigma^*$        | $\Xi^*$           | $\Omega$          |
|----------------------|--------------|-------------------|-------------------|-------------------|-------------------|
| ${}^4 10_J[56, 0^+]$ | (0,0)        | 1246 <sup>†</sup> | 1382 <sup>†</sup> | 1524 <sup>†</sup> | 1670 <sup>†</sup> |
| ${}^2 10_J[70, 1^-]$ | (0,0)        | 1649 <sup>†</sup> | 1755              | 1869              | 1989              |
| ${}^4 10_J[56, 2^+]$ | (0,0)        | 1921 <sup>†</sup> | 2012 <sup>†</sup> | 2112              | 2219              |
| ${}^2 10_J[70, 2^+]$ | (0,0)        | 1946 <sup>‡</sup> | 2037              | 2135              | 2242              |
| ${}^2 10_J[70, 2^-]$ | (0,0)        | 1946 <sup>†</sup> | 2037              | 2135              | 2242              |
| ${}^4 10_J[56, 0^+]$ | (1,0)        | 1660 <sup>†</sup> | 1765              | 1878              | 1998              |
| ${}^2 10_J[70, 1^-]$ | (1,0)        | 1981 <sup>‡</sup> | 2070              | 2167              | 2272              |
| ${}^2 10_J[70, 0^+]$ | (0,1)        | 1764 <sup>‡</sup> | 1863              | 1970              | 2085              |
| ${}^4 10_J[56, 1^-]$ | (0,1)        | 2020              | 2107              | 2203              | 2306              |
| ${}^2 10_J[70, 1^-]$ | (0,1)        | 2044              | 2131              | 2225              | 2327              |
| ${}^2 10_J[70, 1^+]$ | (0,1)        | 2044              | 2131              | 2225              | 2327              |

Table VII: As Table V, but for singlet baryons.

| State               | $(v_1, v_2)$ | $\Lambda^*$ |
|---------------------|--------------|-------------|
| ${}^2 1_J[70, 1^-]$ | (0,0)        | 1641 †      |
| ${}^4 1_J[20, 1^+]$ | (0,0)        | 1891        |
| ${}^2 1_J[70, 2^+]$ | (0,0)        | 1939        |
| ${}^2 1_J[70, 2^-]$ | (0,0)        | 1939        |
| ${}^2 1_J[70, 1^-]$ | (1,0)        | 1974        |
| ${}^4 1_J[20, 1^+]$ | (1,0)        | 2186        |
| ${}^2 1_J[70, 0^+]$ | (0,1)        | 1756        |
| ${}^2 1_J[70, 1^-]$ | (0,1)        | 2038        |
| ${}^2 1_J[70, 1^+]$ | (0,1)        | 2038        |
| ${}^4 1_J[20, 1^-]$ | (0,1)        | 2244        |

Table VIII: Collective form factors in the large  $N$  limit. The states are labeled by  $[dim, L^P]_{(v_1, v_2)}$ , where  $dim$  denotes the dimension of the  $SU_{\text{sf}}(6)$  representation. The final state is  $[56, 0^+]_{(0,0)}$ . The form factors for vibrational excitations are proportional to the coefficients  $\chi_1$  and  $\chi_2$  [5].  $H(x) = \arctan x - x/(1+x^2)$ .

| Initial state       | $\mathcal{F}(k)$   |
|---------------------|--|
| $[56, 0^+]_{(0,0)}$ | $\frac{1}{(1+k^2 a^2)^2}$  |
| $[20, 1^+]_{(0,0)}$ | 0  |
| $[70, 1^-]_{(0,0)}$ | $i\sqrt{3} \frac{ka}{(1+k^2 a^2)^2}$   |
| $[56, 2^+]_{(0,0)}$ | $\frac{1}{2}\sqrt{5} \left[ \frac{-1}{(1+k^2 a^2)^2} + \frac{3}{2k^3 a^3} H(ka) \right]$   |
| $[70, 2^-]_{(0,0)}$ | 0  |
| $[70, 2^+]_{(0,0)}$ | $-\frac{1}{2}\sqrt{15} \left[ \frac{-1}{(1+k^2 a^2)^2} + \frac{3}{2k^3 a^3} H(ka) \right]$ |
| $[56, 0^+]_{(1,0)}$ | $-\chi_1 \frac{2k^2 a^2}{(1+k^2 a^2)^3}$   |
| $[20, 1^+]_{(1,0)}$ | 0  |
| $[70, 1^-]_{(1,0)}$ | $i\chi_1 \sqrt{3} \frac{ka(1-3k^2 a^2)}{2(1+k^2 a^2)^3}$                                   |
| $[70, 0^+]_{(0,1)}$ | $\chi_2 \frac{2k^2 a^2}{(1+k^2 a^2)^3}$  |
| $[70, 1^+]_{(0,1)}$ | 0  |
| $[56, 1^-]_{(0,1)}$ | $-i\chi_2 \sqrt{6} \frac{k^3 a^3}{(1+k^2 a^2)^3}$  |
| $[20, 1^-]_{(0,1)}$ | 0  |
| $[70, 1^-]_{(0,1)}$ | $-i\chi_2 \sqrt{\frac{3}{2}} \frac{ka(1-k^2 a^2)}{(1+k^2 a^2)^3}$                          |

Table IX: Coefficients  $\alpha_{m,\gamma}$  ( $m = 0, \pm$ ) of Eq. (5.12) for strong decay of baryons  $B \rightarrow B_8 + M_8$  where  $B_8$  is an octet ground state baryon with  ${}^28[56]$  and  $M_8$  an octet meson.

| B            | Helicity $\nu = 1/2$          |                       |                                |                        |                                |                        |
|--------------|-------------------------------|-----------------------|--------------------------------|------------------------|--------------------------------|------------------------|
|              | $\alpha_{-, \gamma}$          |                       | $\alpha_{0, \gamma}$           |                        | $\alpha_{+, \gamma}$           |                        |
| ${}^28[56]$  | 0                             | 0                     | $\frac{\sqrt{5}}{3\sqrt{3}}$   | $\frac{2}{3\sqrt{3}}$  | $\frac{2\sqrt{5}}{3\sqrt{3}}$  | $\frac{4}{3\sqrt{3}}$  |
| ${}^28[70]$  | 0                             | 0                     | $\frac{\sqrt{5}}{6\sqrt{6}}$   | $\frac{5}{6\sqrt{6}}$  | $\frac{\sqrt{5}}{3\sqrt{6}}$   | $\frac{5}{3\sqrt{6}}$  |
| ${}^48[70]$  | $-\frac{\sqrt{5}}{3\sqrt{2}}$ | $\frac{1}{3\sqrt{2}}$ | $\frac{\sqrt{5}}{3\sqrt{6}}$   | $-\frac{1}{3\sqrt{6}}$ | $\frac{\sqrt{5}}{3\sqrt{6}}$   | $-\frac{1}{3\sqrt{6}}$ |
| ${}^28[20]$  | 0                             | 0                     | 0                              | 0                      | 0                              | 0                      |
| ${}^410[56]$ | $\frac{2\sqrt{2}}{3}$         |                       | $-\frac{2\sqrt{2}}{3\sqrt{3}}$ |                        | $-\frac{2\sqrt{2}}{3\sqrt{3}}$ |                        |
| ${}^210[70]$ | 0                             |                       | $-\frac{1}{3\sqrt{6}}$         |                        | $-\frac{\sqrt{2}}{3\sqrt{3}}$  |                        |
| ${}^21[70]$  | 0                             |                       | $-\frac{1}{\sqrt{3}}$          |                        | $-\frac{2}{\sqrt{3}}$          |                        |
| ${}^41[20]$  | 0                             |                       | 0                              |                        | 0                              |                        |

Table X: Coefficients  $\alpha_{m,\gamma}$  ( $m = 0, \pm$ ) of Eq. (5.12) for strong decay of baryons  $B \rightarrow B_{10} + M_8$  where  $B_{10}$  is an decuplet ground state baryon with  ${}^4 10[56]$  and  $M_8$  an octet meson.

| B             | Helicity $\nu = 1/2$  |                                |                                | Helicity $\nu = 3/2$ |                               |                        |
|---------------|-----------------------|--------------------------------|--------------------------------|----------------------|-------------------------------|------------------------|
|               | $\alpha_{-, \gamma}$  | $\alpha_{0, \gamma}$           | $\alpha_{+, \gamma}$           | $\alpha_{-, \gamma}$ | $\alpha_{0, \gamma}$          | $\alpha_{+, \gamma}$   |
| ${}^2 8[56]$  | 0                     | $\frac{\sqrt{10}}{3\sqrt{3}}$  | $-\frac{\sqrt{10}}{3\sqrt{3}}$ | 0                    | 0                             | $-\frac{\sqrt{10}}{3}$ |
| ${}^2 8[70]$  | 0                     | $-\frac{\sqrt{5}}{3\sqrt{3}}$  | $\frac{\sqrt{5}}{3\sqrt{3}}$   | 0                    | 0                             | $\frac{\sqrt{5}}{3}$   |
| ${}^4 8[70]$  | $-\frac{\sqrt{5}}{3}$ | $-\frac{\sqrt{5}}{6\sqrt{3}}$  | $-\frac{2\sqrt{5}}{3\sqrt{3}}$ | 0                    | $-\frac{\sqrt{5}}{2\sqrt{3}}$ | $-\frac{\sqrt{5}}{3}$  |
| ${}^2 8[20]$  | 0                     | 0                              | 0                              | 0                    | 0                             | 0                      |
| ${}^4 10[56]$ | $\frac{2\sqrt{2}}{3}$ | $\frac{\sqrt{2}}{3\sqrt{3}}$   | $\frac{4\sqrt{2}}{3\sqrt{3}}$  | 0                    | $\frac{\sqrt{2}}{\sqrt{3}}$   | $\frac{2\sqrt{2}}{3}$  |
| ${}^2 10[70]$ | 0                     | $-\frac{2\sqrt{2}}{3\sqrt{3}}$ | $\frac{2\sqrt{2}}{3\sqrt{3}}$  | 0                    | 0                             | $\frac{2\sqrt{2}}{3}$  |



Table XI: Coefficients  $\alpha_{m,\gamma}$  ( $m = 0, \pm$ ) of Eq. (5.12) for strong decay of baryons  $B \rightarrow B_8 + M_1$  where  $B_8$  is an octet ground state baryon with  ${}^28[56]$  and  $M_1$  a singlet meson.

| B           | Helicity $\nu = 1/2$ |                        |                              |
|-------------|----------------------|------------------------|------------------------------|
|             | $\alpha_{-, \gamma}$ | $\alpha_{0, \gamma}$   | $\alpha_{+, \gamma}$         |
| ${}^28[56]$ | 0                    | $\frac{1}{3\sqrt{6}}$  | $\frac{\sqrt{2}}{3\sqrt{3}}$ |
| ${}^28[70]$ | 0                    | $\frac{1}{3\sqrt{3}}$  | $\frac{2}{3\sqrt{3}}$        |
| ${}^48[70]$ | $\frac{1}{3}$        | $-\frac{1}{3\sqrt{3}}$ | $-\frac{1}{3\sqrt{3}}$       |
| ${}^28[20]$ | 0                    | 0                      | 0                            |

Table XII: Coefficients  $\alpha_{m,\gamma}$  ( $m = 0, \pm$ ) of Eq. (5.12) for strong decay of baryons  $B \rightarrow B_{10} + M_1$  where  $B_{10}$  is an decuplet ground state baryon with  ${}^410[56]$  and  $M_1$  a singlet meson.

| B            | Helicity $\nu = 1/2$ |                               |                               | Helicity $\nu = 3/2$ |                      |                      |
|--------------|----------------------|-------------------------------|-------------------------------|----------------------|----------------------|----------------------|
|              | $\alpha_{-, \gamma}$ | $\alpha_{0, \gamma}$          | $\alpha_{+, \gamma}$          | $\alpha_{-, \gamma}$ | $\alpha_{0, \gamma}$ | $\alpha_{+, \gamma}$ |
| ${}^410[56]$ | $\frac{\sqrt{2}}{3}$ | $\frac{1}{3\sqrt{6}}$         | $\frac{2\sqrt{2}}{3\sqrt{3}}$ | 0                    | $\frac{1}{\sqrt{6}}$ | $\frac{\sqrt{2}}{3}$ |
| ${}^210[70]$ | 0                    | $-\frac{\sqrt{2}}{3\sqrt{3}}$ | $\frac{\sqrt{2}}{3\sqrt{3}}$  | 0                    | 0                    | $\frac{\sqrt{2}}{3}$ |

Table XIII: Strong decay widths of three and four star nucleon resonances in MeV. The experimental values are taken from [13]. Decay channels labeled by – are below threshold.

| Baryon            | $N\pi$              | $N\eta$          | $\Sigma K$ | $\Lambda K$      | $\Delta\pi$        | $\Sigma^* K$ |
|-------------------|---------------------|------------------|------------|------------------|--------------------|--------------|
| $N(1440)P_{11}$   | 108<br>$227 \pm 67$ | –                | –          | –                | 0<br>$87 \pm 30$   | –            |
| $N(1520)D_{13}$   | 115<br>$67 \pm 9$   | 1                | –          | –                | 12<br>$24 \pm 7$   | –            |
| $N(1535)S_{11}$   | 85<br>$79 \pm 38$   | 0<br>$74 \pm 39$ | –          | –                | 23<br>$< 1 \pm 1$  | –            |
| $N(1650)S_{11}$   | 35<br>$121 \pm 34$  | 8<br>$11 \pm 6$  | –          | 0<br>$12 \pm 7$  | 24<br>$7 \pm 5$    | –            |
| $N(1675)D_{15}$   | 31<br>$72 \pm 12$   | 17               | –          | 0<br>$< 1 \pm 1$ | 123<br>$88 \pm 14$ | –            |
| $N(1680)F_{15}$   | 41<br>$84 \pm 9$    | 0                | –          | 0                | 5<br>$13 \pm 7$    | –            |
| $N(1700)D_{13}$   | 5<br>$10 \pm 7$     | 4                | 0          | 0<br>$< 2 \pm 2$ | 225                | –            |
| $N(1710)P_{11}$   | 85<br>$23 \pm 17$   | 8                | 0          | 1<br>$23 \pm 21$ | 34<br>$41 \pm 33$  | –            |
| $N(1720)P_{13}$   | 31<br>$23 \pm 11$   | 0                | 0          | 0<br>$12 \pm 11$ | 10                 | –            |
| $N(2190)G_{17}$   | 34<br>$68 \pm 27$   | 11               | 1          | 7                | 25                 | 1            |
| $N(2220)H_{19}$   | 15<br>$65 \pm 28$   | 1                | 0          | 2                | 5                  | 0            |
| $N(2250)G_{19}$   | 7<br>$38 \pm 21$    | 9                | 9          | 0                | 40                 | 2            |
| $N(2600)I_{1,11}$ | 9<br>$49 \pm 20$    | 3                | 0          | 3                | 7                  | 1            |

Table XIV: As Table XIII, but for  $\Delta$  resonances.

| Baryon                 | $N\pi$             | $\Sigma K$ | $\Delta\pi$         | $\Delta\eta$ | $\Sigma^*K$ |
|------------------------|--------------------|------------|---------------------|--------------|-------------|
| $\Delta(1232)P_{33}$   | 116<br>$119 \pm 5$ | –          | –                   | –            | –           |
| $\Delta(1600)P_{33}$   | 108<br>$61 \pm 32$ | –          | 25<br>$193 \pm 76$  | –            | –           |
| $\Delta(1620)S_{31}$   | 16<br>$38 \pm 11$  | –          | 89<br>$68 \pm 26$   | –            | –           |
| $\Delta(1700)D_{33}$   | 27<br>$45 \pm 21$  | 0          | 144<br>$135 \pm 64$ | –            | –           |
| $\Delta(1905)F_{35}$   | 9<br>$36 \pm 20$   | 1          | 45<br>$< 45 \pm 45$ | 1            | 0           |
| $\Delta(1910)P_{31}$   | 42<br>$52 \pm 19$  | 2          | 4                   | 0            | 0           |
| $\Delta(1920)P_{33}$   | 22<br>$28 \pm 19$  | 1          | 29                  | 1            | 0           |
| $\Delta(1930)D_{35}$   | 0<br>$53 \pm 23$   | 0          | 0                   | 0            | 0           |
| $\Delta(1950)F_{37}$   | 45<br>$120 \pm 14$ | 6          | 36<br>$80 \pm 18$   | 2            | 0           |
| $\Delta(2420)H_{3,11}$ | 12<br>$40 \pm 22$  | 4          | 11                  | 2            | 1           |

Table XV: As Table XIII, but for  $\Sigma$  resonances.

| Baryon                 | $N\bar{K}$         | $\Sigma\pi$       | $\Lambda\pi$     | $\Sigma\eta$     | $\Xi K$          | $\Delta\bar{K}$   | $\Sigma^*\pi$    | $\Sigma^*\eta$ | $\Xi^*K$ |
|------------------------|--------------------|-------------------|------------------|------------------|------------------|-------------------|------------------|----------------|----------|
| $\Sigma(1660)P_{11}$   | 2<br>$24 \pm 20$   | 40<br>seen        | 29<br>seen       | –                | –                | –                 | 1                | –              | –        |
| $\Sigma(1670)D_{13}$   | 3<br>$6 \pm 3$     | 77<br>$27 \pm 13$ | 7<br>$6 \pm 4$   | –                | –                | –                 | 2                | –              | –        |
| $\Sigma(1750)S_{11}$   | 3<br>$28 \pm 21$   | 85<br>$< 4 \pm 4$ | 7<br>seen        | 0<br>$39 \pm 28$ | –                | 1                 | 10               | –              | –        |
| $\Sigma(1775)D_{15}$   | 58<br>$48 \pm 7$   | 14<br>$4 \pm 2$   | 27<br>$20 \pm 4$ | 0                | –                | 4                 | 14<br>$12 \pm 3$ | –              | –        |
| $\Sigma(1915)F_{15}$   | 1<br>$12 \pm 7$    | 20<br>seen        | 10<br>seen       | 1                | 1                | 3                 | 2<br>$< 3 \pm 3$ | –              | –        |
| $\Sigma(1940)D_{13}$   | 2<br>$< 23 \pm 23$ | 30<br>seen        | 16<br>seen       | 1                | 0                | 4<br>seen         | 3<br>seen        | 0              | –        |
| $\Sigma^*(1385)P_{13}$ | –                  | 9<br>$4 \pm 1$    | 49<br>$32 \pm 4$ | –                | –                | –                 | –                | –              | –        |
| $\Sigma^*(2030)F_{17}$ | 12<br>$35 \pm 7$   | 11<br>$13 \pm 5$  | 19<br>$35 \pm 7$ | 5                | 1<br>$< 2 \pm 2$ | 10<br>$26 \pm 10$ | 14<br>$18 \pm 9$ | 0              | 0        |

Table XVI: As Table XIII, but for  $\Lambda$  resonances.

| Baryon                  | $N\bar{K}$        | $\Sigma\pi$          | $\Lambda\eta$    | $\Xi K$          | $\Sigma^*\pi$       | $\Xi^*K$ |
|-------------------------|-------------------|----------------------|------------------|------------------|---------------------|----------|
| $\Lambda(1600)P_{01}$   | 25<br>$34 \pm 25$ | 21<br>$53 \pm 51$    | –                | –                | 0                   | –        |
| $\Lambda(1670)S_{01}$   | 44<br>$8 \pm 3$   | 9<br>$15 \pm 9$      | 0<br>$9 \pm 5$   | –                | 14                  | –        |
| $\Lambda(1690)D_{03}$   | 100<br>$15 \pm 4$ | 16<br>$18 \pm 7$     | 0                | –                | 14                  | –        |
| $\Lambda(1800)S_{01}$   | 0<br>$98 \pm 40$  | 80<br>seen           | 5                | –                | 19<br>seen          | –        |
| $\Lambda(1810)P_{01}$   | 62<br>$53 \pm 42$ | 9<br>$38 \pm 34$     | 0                | –                | 15<br>seen          | –        |
| $\Lambda(1820)F_{05}$   | 23<br>$48 \pm 7$  | 13<br>$9 \pm 3$      | 0                | 0                | 3<br>$6 \pm 2$      | –        |
| $\Lambda(1830)D_{05}$   | 0<br>$6 \pm 3$    | 77<br>$47 \pm 22$    | 16               | 0                | 101<br>$> 13 \pm 4$ | –        |
| $\Lambda(1890)P_{03}$   | 19<br>$36 \pm 22$ | 12<br>$8 \pm 6$      | 0                | 0                | 10<br>seen          | –        |
| $\Lambda(2110)F_{05}$   | 0<br>$30 \pm 21$  | 10<br>$50 \pm 33$    | 4                | 2                | 120<br>seen         | 1        |
| $\Lambda^*(1405)S_{01}$ | –                 | 0<br>$50 \pm 2$      | –                | –                |                     |          |
| $\Lambda^*(1520)D_{03}$ | 10<br>$7 \pm 1$   | 28<br>$7 \pm 1$      | –                | –                |                     |          |
| $\Lambda^*(2100)G_{07}$ | 18<br>$53 \pm 24$ | 22<br>$\sim 9 \pm 4$ | 4<br>$< 3 \pm 3$ | 2<br>$< 3 \pm 3$ |                     |          |

Table XVII: As Table XIII, but for  $\Xi$  resonances.

| Baryon              | $\Sigma\bar{K}$ | $\Lambda\bar{K}$ | $\Xi\pi$         | $\Xi\eta$ | $\Sigma^*\bar{K}$ | $\Xi^*\pi$     | $\Xi^*\eta$ | $\Omega K$ |
|---------------------|-----------------|------------------|------------------|-----------|-------------------|----------------|-------------|------------|
| $\Xi(1820)D_{13}$   | 30<br>$7 \pm 4$ | 18<br>$7 \pm 4$  | 6<br>$2 \pm 2$   | –         | –                 | 3<br>$7 \pm 4$ | –           | –          |
| $\Xi^*(1530)P_{13}$ | –               | –                | 22<br>$10 \pm 1$ | –         | –                 | –              | –           | –          |

Table XVIII: Strong decay widths of missing nucleon resonances in MeV. Tentative assignments of one and two star resonances are labeled by ‡.

| $N$                     | $(v_1, v_2)$ | Mass   | $N\pi$ | $N\eta$ | $\Sigma K$ | $\Lambda K$ | $\Delta\pi$ | $\Sigma^* K$ |
|-------------------------|--------------|--------|--------|---------|------------|-------------|-------------|--------------|
| ${}^2 8_J[20, 1^+]$     | (0,0)        | 1713   | 0      | 0       | 0          | 0           | 0           | –            |
| ${}^2 8_{3/2}[70, 2^+]$ | (0,0)        | 1874 ‡ | 56     | 9       | 0          | 3           | 56          | –            |
| ${}^2 8_{5/2}[70, 2^+]$ | (0,0)        | 1874   | 84     | 19      | 0          | 8           | 43          | –            |
| ${}^2 8_J[70, 2^-]$     | (0,0)        | 1874   | 0      | 0       | 0          | 0           | 0           | –            |
| ${}^4 8_{1/2}[70, 2^+]$ | (0,0)        | 1975   | 19     | 18      | 7          | 0           | 16          | 0            |
| ${}^4 8_{3/2}[70, 2^+]$ | (0,0)        | 1975   | 10     | 9       | 4          | 0           | 96          | 0            |
| ${}^4 8_{5/2}[70, 2^+]$ | (0,0)        | 1975 ‡ | 4      | 5       | 3          | 0           | 159         | 0            |
| ${}^4 8_{7/2}[70, 2^+]$ | (0,0)        | 1975 ‡ | 18     | 20      | 12         | 0           | 98          | 0            |
| ${}^4 8_J[70, 2^-]$     | (0,0)        | 1975   | 0      | 0       | 0          | 0           | 0           | 0            |
| ${}^2 8_{1/2}[70, 1^-]$ | (1,0)        | 1909   | 22     | 1       | 0          | 0           | 1           | 0            |
| ${}^2 8_{3/2}[70, 1^-]$ | (1,0)        | 1909   | 28     | 1       | 0          | 0           | 1           | 0            |
| ${}^4 8_{1/2}[70, 1^-]$ | (1,0)        | 2009   | 10     | 4       | 0          | 0           | 3           | 0            |
| ${}^4 8_{3/2}[70, 1^-]$ | (1,0)        | 2009   | 1      | 1       | 0          | 0           | 21          | 2            |
| ${}^4 8_{5/2}[70, 1^-]$ | (1,0)        | 2009   | 8      | 4       | 0          | 0           | 13          | 2            |
| ${}^2 8_J[20, 1^+]$     | (1,0)        | 2034   | 0      | 0       | 0          | 0           | 0           | 0            |
| ${}^4 8_{3/2}[70, 0^+]$ | (0,1)        | 1796   | 14     | 10      | 1          | 0           | 91          | –            |
| ${}^2 8_{1/2}[56, 1^-]$ | (0,1)        | 1847   | 96     | 2       | 0          | 1           | 35          | –            |
| ${}^2 8_{3/2}[56, 1^-]$ | (0,1)        | 1847   | 123    | 3       | 0          | 3           | 30          | –            |
| ${}^2 8_{1/2}[70, 1^-]$ | (0,1)        | 1975   | 2      | 3       | 0          | 4           | 18          | 2            |
| ${}^2 8_{3/2}[70, 1^-]$ | (0,1)        | 1975   | 2      | 4       | 1          | 6           | 16          | 1            |
| ${}^2 8_J[70, 1^+]$     | (0,1)        | 1975   | 0      | 0       | 0          | 0           | 0           | 0            |
| ${}^4 8_{1/2}[70, 1^-]$ | (0,1)        | 2072   | 0      | 2       | 7          | 0           | 3           | 1            |
| ${}^4 8_{3/2}[70, 1^-]$ | (0,1)        | 2072   | 0      | 0       | 1          | 0           | 22          | 6            |
| ${}^4 8_{5/2}[70, 1^-]$ | (0,1)        | 2072   | 0      | 1       | 6          | 0           | 13          | 5            |
| ${}^4 8_J[70, 1^+]$     | (0,1)        | 2072   | 0      | 0       | 0          | 0           | 0           | 0            |
| ${}^2 8_J[20, 1^-]$     | (0,1)        | 2096   | 0      | 0       | 0          | 0           | 0           | 0            |



Table XIX: As Table XVIII, but for missing  $\Sigma$  resonances.

| $\Sigma$              | $(v_1, v_2)$ | Mass              | $N\bar{K}$ | $\Sigma\pi$ | $\Lambda\pi$ | $\Sigma\eta$ | $\Xi K$ | $\Delta\bar{K}$ | $\Sigma^*\pi$ | $\Sigma^*\eta$ | $\Xi^*K$ |
|-----------------------|--------------|-------------------|------------|-------------|--------------|--------------|---------|-----------------|---------------|----------------|----------|
| $^4 8_{1/2}[70, 1^-]$ | (0,0)        | 1822              | 78         | 20          | 39           | 0            | 0       | 5               | 5             | -              | -        |
| $^4 8_{3/2}[70, 1^-]$ | (0,0)        | 1822              | 12         | 3           | 5            | 0            | 0       | 20              | 31            | -              | -        |
| $^2 8_J[20, 1^+]$     | (0,0)        | 1849              | 0          | 0           | 0            | 0            | 0       | 0               | 0             | -              | -        |
| $^2 8_{3/2}[56, 2^+]$ | (0,0)        | 1872              | 1          | 9           | 5            | 0            | 0       | 2               | 2             | -              | -        |
| $^2 8_{3/2}[70, 2^+]$ | (0,0)        | 1999              | 2          | 43          | 3            | 1            | 1       | 21              | 9             | 0              | -        |
| $^2 8_{5/2}[70, 2^+]$ | (0,0)        | 1999              | 3          | 68          | 5            | 4            | 4       | 14              | 7             | 0              | -        |
| $^2 8_J[70, 2^-]$     | (0,0)        | 1999              | 0          | 0           | 0            | 0            | 0       | 0               | 0             | 0              | -        |
| $^4 8_{1/2}[70, 2^+]$ | (0,0)        | 2095              | 43         | 10          | 19           | 1            | 1       | 6               | 2             | 0              | 0        |
| $^4 8_{3/2}[70, 2^+]$ | (0,0)        | 2095              | 22         | 5           | 9            | 0            | 1       | 41              | 15            | 0              | 0        |
| $^4 8_{5/2}[70, 2^+]$ | (0,0)        | 2095              | 10         | 2           | 4            | 0            | 0       | 70              | 25            | 1              | 0        |
| $^4 8_{7/2}[70, 2^+]$ | (0,0)        | 2095              | 43         | 10          | 18           | 1            | 2       | 47              | 15            | 1              | 0        |
| $^4 8_J[70, 2^-]$     | (0,0)        | 2095              | 0          | 0           | 0            | 0            | 0       | 0               | 0             | 0              | 0        |
| $^2 8_{1/2}[70, 1^-]$ | (1,0)        | 2033              | 1          | 10          | 1            | 0            | 1       | 0               | 0             | 0              | 0        |
| $^2 8_{3/2}[70, 1^-]$ | (1,0)        | 2033              | 1          | 14          | 2            | 0            | 2       | 0               | 0             | 0              | 0        |
| $^4 8_{1/2}[70, 1^-]$ | (1,0)        | 2127              | 22         | 4           | 9            | 0            | 0       | 1               | 0             | 0              | 0        |
| $^4 8_{3/2}[70, 1^-]$ | (1,0)        | 2127              | 3          | 1           | 1            | 0            | 0       | 3               | 2             | 1              | 1        |
| $^4 8_{5/2}[70, 1^-]$ | (1,0)        | 2127              | 18         | 3           | 7            | 0            | 0       | 2               | 2             | 0              | 1        |
| $^2 8_J[20, 1^+]$     | (1,0)        | 2150              | 0          | 0           | 0            | 0            | 0       | 0               | 0             | 0              | 0        |
| $^2 8_{1/2}[70, 0^+]$ | (0,1)        | 1822 <sup>‡</sup> | 2          | 56          | 5            | 0            | 0       | 1               | 4             | -              | -        |
| $^4 8_{3/2}[70, 0^+]$ | (0,1)        | 1926              | 31         | 7           | 14           | 0            | 0       | 23              | 14            | -              | -        |
| $^2 8_{1/2}[56, 1^-]$ | (0,1)        | 1974              | 2          | 27          | 15           | 1            | 0       | 9               | 5             | 0              | -        |
| $^2 8_{1/2}[70, 1^-]$ | (0,1)        | 2095              | 0          | 4           | 0            | 2            | 5       | 13              | 3             | 1              | 1        |
| $^2 8_{3/2}[70, 1^-]$ | (0,1)        | 2095              | 0          | 4           | 0            | 3            | 7       | 11              | 3             | 1              | 0        |
| $^2 8_J[70, 1^+]$     | (0,1)        | 2095              | 0          | 0           | 0            | 0            | 0       | 0               | 0             | 0              | 0        |
| $^4 8_{1/2}[70, 1^-]$ | (0,1)        | 2186              | 0          | 0           | 0            | 0            | 1       | 2               | 1             | 0              | 1        |
| $^4 8_{3/2}[70, 1^-]$ | (0,1)        | 2186              | 0          | 0           | 0            | 0            | 0       | 17              | 4             | 2              | 3        |
| $^4 8_{5/2}[70, 1^-]$ | (0,1)        | 2186              | 0          | 0           | 0            | 0            | 1       | 10              | 2             | 1              | 3        |
| $^4 8_J[70, 1^+]$     | (0,1)        | 2186              | 0          | 0           | 0            | 0            | 0       | 0               | 0             | 0              | 0        |
| $^2 8_J[20, 1^-]$     | (0,1)        | 2209              | 0          | 0           | 0            | 0            | 0       | 0               | 0             | 0              | 0        |

Table XX: As Table XVIII, but for missing  $\Lambda$  resonances.

| $\Lambda$                     | $(v_1, v_2)$ | Mass | $N\bar{K}$ | $\Sigma\pi$ | $\Lambda\eta$ | $\Xi K$ | $\Sigma^*\pi$ | $\Xi^*K$ |
|-------------------------------|--------------|------|------------|-------------|---------------|---------|---------------|----------|
| $^4\mathbf{8}_{3/2}[70, 1^-]$ | (0,0)        | 1799 | 0          | 11          | 2             | –       | 112           | –        |
| $^2\mathbf{8}_J[20, 1^+]$     | (0,0)        | 1826 | 0          | 0           | 0             | 0       | 0             | –        |
| $^2\mathbf{8}_{3/2}[70, 2^+]$ | (0,0)        | 1978 | 46         | 7           | 0             | 0       | 33            | –        |
| $^2\mathbf{8}_{5/2}[70, 2^+]$ | (0,0)        | 1978 | 77         | 11          | 0             | 2       | 25            | –        |
| $^2\mathbf{8}_J[70, 2^-]$     | (0,0)        | 1978 | 0          | 0           | 0             | 0       | 0             | –        |
| $^4\mathbf{8}_{1/2}[70, 2^+]$ | (0,0)        | 2074 | 0          | 43          | 13            | 3       | 9             | 0        |
| $^4\mathbf{8}_{3/2}[70, 2^+]$ | (0,0)        | 2074 | 0          | 21          | 7             | 2       | 59            | 0        |
| $^4\mathbf{8}_{7/2}[70, 2^+]$ | (0,0)        | 2074 | 0          | 42          | 17            | 5       | 62            | 0        |
| $^4\mathbf{8}_J[70, 2^-]$     | (0,0)        | 2074 | 0          | 0           | 0             | 0       | 0             | 0        |
| $^2\mathbf{8}_{1/2}[70, 1^-]$ | (1,0)        | 2012 | 14         | 1           | 0             | 1       | 0             | –        |
| $^2\mathbf{8}_{3/2}[70, 1^-]$ | (1,0)        | 2012 | 20         | 2           | 0             | 2       | 0             | –        |
| $^4\mathbf{8}_{1/2}[70, 1^-]$ | (1,0)        | 2107 | 0          | 16          | 2             | 0       | 1             | 1        |
| $^4\mathbf{8}_{3/2}[70, 1^-]$ | (1,0)        | 2107 | 0          | 2           | 0             | 0       | 7             | 2        |
| $^4\mathbf{8}_{5/2}[70, 1^-]$ | (1,0)        | 2107 | 0          | 12          | 2             | 0       | 4             | 2        |
| $^2\mathbf{8}_J[20, 1^+]$     | (1,0)        | 2130 | 0          | 0           | 0             | 0       | 0             | 0        |
| $^4\mathbf{8}_{3/2}[70, 0^+]$ | (0,1)        | 1904 | 0          | 30          | 7             | 0       | 52            | –        |
| $^2\mathbf{8}_{1/2}[56, 1^-]$ | (0,1)        | 1952 | 47         | 27          | 1             | 0       | 19            | –        |
| $^2\mathbf{8}_{3/2}[56, 1^-]$ | (0,1)        | 1952 | 66         | 36          | 1             | 0       | 16            | –        |
| $^2\mathbf{8}_{1/2}[70, 1^-]$ | (0,1)        | 2074 | 3          | 1           | 0             | 3       | 15            | 1        |
| $^2\mathbf{8}_{3/2}[70, 1^-]$ | (0,1)        | 2074 | 3          | 1           | 0             | 5       | 13            | 0        |
| $^2\mathbf{8}_J[70, 1^+]$     | (0,1)        | 2074 | 0          | 0           | 0             | 0       | 0             | 0        |
| $^4\mathbf{8}_{1/2}[70, 1^-]$ | (0,1)        | 2167 | 0          | 1           | 2             | 4       | 3             | 2        |
| $^4\mathbf{8}_{3/2}[70, 1^-]$ | (0,1)        | 2167 | 0          | 0           | 0             | 1       | 20            | 8        |
| $^4\mathbf{8}_{5/2}[70, 1^-]$ | (0,1)        | 2167 | 0          | 1           | 2             | 3       | 12            | 7        |
| $^4\mathbf{8}_J[70, 1^+]$     | (0,1)        | 2167 | 0          | 0           | 0             | 0       | 0             | 0        |
| $^2\mathbf{8}_J[20, 1^-]$     | (0,1)        | 2190 | 0          | 0           | 0             | 0       | 0             | 0        |

Table XXI: As Table XVIII, but for missing  $\Xi$  resonances.

| $\Xi$                       | $(v_1, v_2)$ | Mass | $\Sigma\bar{K}$ | $\Lambda\bar{K}$ | $\Xi\pi$ | $\Xi\eta$ | $\Sigma^*\bar{K}$ | $\Xi^*\pi$ | $\Xi^*\eta$ | $\Omega K$ |
|-----------------------------|--------------|------|-----------------|------------------|----------|-----------|-------------------|------------|-------------|------------|
| ${}^2\delta_{1/2}[70, 1^-]$ | (0,0)        | 1828 | 11              | 10               | 4        | –         | –                 | 6          | –           | –          |
| ${}^4\delta_{1/2}[70, 1^-]$ | (0,0)        | 1932 | 14              | 24               | 119      | 0         | 1                 | 6          | –           | –          |
| ${}^4\delta_{3/2}[70, 1^-]$ | (0,0)        | 1932 | 3               | 4                | 17       | 0         | 2                 | 34         | –           | –          |
| ${}^4\delta_{5/2}[70, 1^-]$ | (0,0)        | 1932 | 15              | 23               | 100      | 0         | 2                 | 24         | –           | –          |
| ${}^2\delta_J[20, 1^+]$     | (0,0)        | 1957 | 0               | 0                | 0        | 0         | 0                 | 0          | –           | –          |
| ${}^2\delta_{3/2}[56, 2^+]$ | (0,0)        | 1979 | 8               | 1                | 1        | 0         | 0                 | 2          | –           | –          |
| ${}^2\delta_{5/2}[56, 2^+]$ | (0,0)        | 1979 | 20              | 1                | 1        | 0         | 0                 | 1          | –           | –          |
| ${}^2\delta_{3/2}[70, 2^+]$ | (0,0)        | 2100 | 25              | 9                | 3        | 1         | 5                 | 10         | 0           | –          |
| ${}^2\delta_{5/2}[70, 2^+]$ | (0,0)        | 2100 | 47              | 16               | 4        | 2         | 3                 | 7          | 0           | –          |
| ${}^2\delta_J[70, 2^-]$     | (0,0)        | 2100 | 0               | 0                | 0        | 0         | 0                 | 0          | 0           | –          |
| ${}^4\delta_{1/2}[70, 2^+]$ | (0,0)        | 2191 | 11              | 14               | 60       | 1         | 2                 | 3          | 0           | 0          |
| ${}^4\delta_{3/2}[70, 2^+]$ | (0,0)        | 2191 | 5               | 7                | 30       | 1         | 11                | 18         | 0           | 0          |
| ${}^4\delta_{5/2}[70, 2^+]$ | (0,0)        | 2191 | 3               | 3                | 13       | 0         | 19                | 30         | 0           | 0          |
| ${}^4\delta_{7/2}[70, 2^+]$ | (0,0)        | 2191 | 12              | 15               | 59       | 2         | 13                | 19         | 0           | 0          |
| ${}^4\delta_J[70, 2^-]$     | (0,0)        | 2191 | 0               | 0                | 0        | 0         | 0                 | 0          | 0           | 0          |
| ${}^2\delta_{1/2}[56, 0^+]$ | (1,0)        | 1727 | 0               | 0                | 2        | –         | –                 | 0          | –           | –          |
| ${}^2\delta_{1/2}[70, 1^-]$ | (1,0)        | 2132 | 3               | 2                | 1        | 0         | 1                 | 0          | 0           | –          |
| ${}^2\delta_{3/2}[70, 1^-]$ | (1,0)        | 2132 | 5               | 3                | 1        | 0         | 1                 | 0          | 0           | –          |
| ${}^4\delta_{1/2}[70, 1^-]$ | (1,0)        | 2222 | 3               | 6                | 22       | 0         | 0                 | 0          | 0           | 0          |
| ${}^4\delta_{3/2}[70, 1^-]$ | (1,0)        | 2222 | 0               | 1                | 3        | 0         | 0                 | 1          | 1           | 1          |
| ${}^4\delta_{5/2}[70, 1^-]$ | (1,0)        | 2222 | 3               | 5                | 17       | 0         | 0                 | 1          | 0           | 1          |
| ${}^2\delta_J[20, 1^+]$     | (1,0)        | 2244 | 0               | 0                | 0        | 0         | 0                 | 0          | 0           | 0          |
| ${}^2\delta_{1/2}[70, 0^+]$ | (0,1)        | 1932 | 24              | 11               | 3        | 0         | 0                 | 4          | –           | –          |
| ${}^4\delta_{3/2}[70, 0^+]$ | (0,1)        | 2030 | 7               | 10               | 44       | 0         | 4                 | 15         | –           | –          |
| ${}^2\delta_{1/2}[56, 1^-]$ | (0,1)        | 2076 | 34              | 2                | 2        | 1         | 2                 | 5          | –           | –          |
| ${}^2\delta_{3/2}[56, 1^-]$ | (0,1)        | 2076 | 52              | 3                | 3        | 1         | 1                 | 4          | –           | –          |
| ${}^2\delta_{1/2}[70, 1^-]$ | (0,1)        | 2191 | 5               | 1                | 0        | 1         | 6                 | 5          | 1           | 0          |
| ${}^2\delta_{3/2}[70, 1^-]$ | (0,1)        | 2191 | 6               | 1                | 0        | 2         | 5                 | 5          | 0           | 0          |
| ${}^2\delta_J[70, 1^+]$     | (0,1)        | 2191 | 0               | 0                | 0        | 0         | 0                 | 0          | 0           | 0          |
| ${}^4\delta_{1/2}[70, 1^-]$ | (0,1)        | 2278 | 1               | 0                | 2        | 0         | 1                 | 1          | 0           | 1          |
| ${}^4\delta_{3/2}[70, 1^-]$ | (0,1)        | 2278 | 0               | 0                | 0        | 0         | 8                 | 8          | 2           | 6          |
| ${}^4\delta_{5/2}[70, 1^-]$ | (0,1)        | 2278 | 0               | 0                | 1        | 0         | 5                 | 4          | 1           | 5          |
| ${}^4\delta_J[70, 1^+]$     | (0,1)        | 2278 | 0               | 0                | 0        | 0         | 0                 | 0          | 0           | 0          |
| ${}^2\delta_J[20, 1^-]$     | (0,1)        | 2300 | 0               | 0                | 0        | 0         | 0                 | 0          | 0           | 0          |

Table XXII: As Table XVIII, but for missing  $\Delta$  resonances.

| $\Delta$                 | $(v_1, v_2)$ | Mass            | $N\pi$ | $\Sigma K$ | $\Delta\pi$ | $\Delta\eta$ | $\Sigma^* K$ |
|--------------------------|--------------|-----------------|--------|------------|-------------|--------------|--------------|
| ${}^2 10_{3/2}[70, 2^+]$ | (0,0)        | 1946            | 9      | 1          | 106         | 5            | 0            |
| ${}^2 10_{5/2}[70, 2^+]$ | (0,0)        | 1946 $\ddagger$ | 13     | 2          | 84          | 3            | 0            |
| ${}^2 10_{3/2}[70, 2^-]$ | (0,0)        | 1946            | 0      | 0          | 0           | 0            | 0            |
| ${}^2 10_{1/2}[70, 1^-]$ | (1,0)        | 1981 $\ddagger$ | 4      | 0          | 9           | 3            | 3            |
| ${}^2 10_{3/2}[70, 1^-]$ | (1,0)        | 1981            | 6      | 0          | 8           | 3            | 2            |
| ${}^2 10_{1/2}[70, 0^+]$ | (0,1)        | 1764 $\ddagger$ | 13     | 0          | 71          | –            | –            |
| ${}^4 10_{1/2}[56, 1^-]$ | (0,1)        | 2020            | 113    | 12         | 18          | 1            | 0            |
| ${}^4 10_{3/2}[56, 1^-]$ | (0,1)        | 2020            | 14     | 2          | 128         | 6            | 0            |
| ${}^4 10_{5/2}[56, 1^-]$ | (0,1)        | 2020            | 84     | 12         | 77          | 4            | 0            |
| ${}^2 10_{1/2}[70, 1^-]$ | (0,1)        | 2044            | 0      | 1          | 17          | 12           | 8            |
| ${}^2 10_{3/2}[70, 1^-]$ | (0,1)        | 2044            | 0      | 1          | 15          | 9            | 5            |
| ${}^2 10_J[70, 1^+]$     | (0,1)        | 2044            | 0      | 0          | 0           | 0            | 0            |

Table XXIII: As Table XVIII, but for missing  $\Sigma^*$  resonances.

| $\Sigma^*$               | $(v_1, v_2)$ | Mass | $N\bar{K}$ | $\Sigma\pi$ | $\Lambda\pi$ | $\Sigma\eta$ | $\Xi K$ | $\Delta\bar{K}$ | $\Sigma^*\pi$ | $\Sigma^*\eta$ | $\Xi^*K$ |
|--------------------------|--------------|------|------------|-------------|--------------|--------------|---------|-----------------|---------------|----------------|----------|
| ${}^2 10_{1/2}[70, 1^-]$ | (0,0)        | 1755 | 3          | 4           | 7            | 0            | –       | 1               | 42            | –              | –        |
| ${}^2 10_{3/2}[70, 1^-]$ | (0,0)        | 1755 | 5          | 5           | 10           | 0            | –       | 1               | 32            | –              | –        |
| ${}^4 10_{1/2}[56, 2^+]$ | (0,0)        | 2012 | 11         | 10          | 19           | 2            | 0       | 1               | 2             | 0              | –        |
| ${}^4 10_{3/2}[56, 2^+]$ | (0,0)        | 2012 | 5          | 5           | 9            | 1            | 0       | 7               | 12            | 0              | –        |
| ${}^4 10_{5/2}[56, 2^+]$ | (0,0)        | 2012 | 2          | 2           | 4            | 1            | 0       | 11              | 20            | 0              | –        |
| ${}^2 10_{3/2}[70, 2^+]$ | (0,0)        | 2037 | 2          | 2           | 4            | 1            | 0       | 30              | 44            | 0              | 0        |
| ${}^2 10_{5/2}[70, 2^+]$ | (0,0)        | 2037 | 4          | 3           | 6            | 1            | 0       | 21              | 34            | 0              | 0        |
| ${}^2 10_J[70, 2^-]$     | (0,0)        | 2037 | 0          | 0           | 0            | 0            | 0       | 0               | 0             | 0              | 0        |
| ${}^4 10_{3/2}[56, 0^+]$ | (1,0)        | 1765 | 28         | 26          | 58           | 0            | –       | 0               | 18            | –              | –        |
| ${}^2 10_{1/2}[70, 1^-]$ | (1,0)        | 2070 | 1          | 1           | 2            | 0            | 0       | 0               | 1             | 1              | 1        |
| ${}^2 10_{3/2}[70, 1^-]$ | (1,0)        | 2070 | 1          | 1           | 2            | 0            | 0       | 0               | 1             | 0              | 0        |
| ${}^2 10_{1/2}[70, 0^+]$ | (0,1)        | 1863 | 3          | 3           | 6            | 0            | 0       | 5               | 25            | –              | –        |
| ${}^4 10_{1/2}[56, 1^-]$ | (0,1)        | 2107 | 29         | 26          | 50           | 10           | 3       | 5               | 7             | 0              | 0        |
| ${}^4 10_{3/2}[56, 1^-]$ | (0,1)        | 2107 | 4          | 3           | 6            | 2            | 0       | 35              | 51            | 0              | 0        |
| ${}^4 10_{5/2}[56, 1^-]$ | (0,1)        | 2107 | 23         | 20          | 37           | 9            | 3       | 23              | 31            | 0              | 0        |
| ${}^2 10_{1/2}[70, 1^-]$ | (0,1)        | 2131 | 0          | 0           | 0            | 0            | 0       | 12              | 12            | 1              | 5        |
| ${}^2 10_{3/2}[70, 1^-]$ | (0,1)        | 2131 | 0          | 0           | 0            | 1            | 0       | 11              | 10            | 1              | 3        |
| ${}^2 10_J[70, 1^+]$     | (0,1)        | 2131 | 0          | 0           | 0            | 0            | 0       | 0               | 0             | 0              | 0        |

Table XXIV: As Table XVIII, but for missing  $\Xi^*$  resonances.

| $\Xi^*$                | $(v_1, v_2)$ | Mass | $\Sigma\bar{K}$ | $\Lambda\bar{K}$ | $\Xi\pi$ | $\Xi\eta$ | $\Sigma^*\bar{K}$ | $\Xi^*\pi$ | $\Xi^*\eta$ | $\Omega K$ |
|------------------------|--------------|------|-----------------|------------------|----------|-----------|-------------------|------------|-------------|------------|
| $^2 10_{1/2}[70, 1^-]$ | (0,0)        | 1869 | 2               | 4                | 5        | 0         | –                 | 11         | –           | –          |
| $^2 10_{3/2}[70, 1^-]$ | (0,0)        | 1869 | 4               | 7                | 8        | 0         | –                 | 8          | –           | –          |
| $^4 10_{1/2}[56, 2^+]$ | (0,0)        | 2112 | 9               | 13               | 14       | 2         | 1                 | 1          | 0           | –          |
| $^4 10_{3/2}[56, 2^+]$ | (0,0)        | 2112 | 4               | 7                | 7        | 1         | 6                 | 3          | 0           | –          |
| $^4 10_{5/2}[56, 2^+]$ | (0,0)        | 2112 | 2               | 3                | 3        | 1         | 10                | 6          | 0           | –          |
| $^4 10_{7/2}[56, 2^+]$ | (0,0)        | 2112 | 11              | 15               | 14       | 3         | 8                 | 4          | 0           | –          |
| $^2 10_{3/2}[70, 2^+]$ | (0,0)        | 2135 | 2               | 3                | 3        | 0         | 30                | 13         | 0           | –          |
| $^2 10_{5/2}[70, 2^+]$ | (0,0)        | 2135 | 4               | 5                | 5        | 1         | 20                | 10         | 0           | –          |
| $^2 10_J[70, 2^-]$     | (0,0)        | 2135 | 0               | 0                | 0        | 0         | 0                 | 0          | 0           | 0          |
| $^4 10_{3/2}[56, 0^+]$ | (1,0)        | 1878 | 12              | 29               | 38       | 0         | –                 | 4          | –           | –          |
| $^2 10_{1/2}[70, 1^-]$ | (1,0)        | 2167 | 0               | 1                | 1        | 0         | 1                 | 0          | 0           | –          |
| $^2 10_{3/2}[70, 1^-]$ | (1,0)        | 2167 | 1               | 1                | 1        | 0         | 1                 | 0          | 0           | –          |
| $^2 10_{1/2}[70, 0^+]$ | (0,1)        | 1970 | 2               | 4                | 4        | 0         | 2                 | 6          | –           | –          |
| $^4 10_{1/2}[56, 1^-]$ | (0,1)        | 2203 | 28              | 38               | 39       | 8         | 5                 | 2          | 0           | 0          |
| $^4 10_{3/2}[56, 1^-]$ | (0,1)        | 2203 | 4               | 5                | 5        | 1         | 34                | 15         | 0           | 0          |
| $^4 10_{5/2}[56, 1^-]$ | (0,1)        | 2203 | 23              | 30               | 30       | 8         | 23                | 9          | 0           | 0          |
| $^2 10_{1/2}[70, 1^-]$ | (0,1)        | 2225 | 0               | 0                | 0        | 0         | 21                | 5          | 0           | 1          |
| $^2 10_{3/2}[70, 1^-]$ | (0,1)        | 2225 | 0               | 0                | 0        | 1         | 18                | 4          | 0           | 1          |
| $^2 10_J[70, 1^+]$     | (0,1)        | 2225 | 0               | 0                | 0        | 0         | 0                 | 0          | 0           | 0          |

Table XXV: As Table XVIII, but for missing  $\Omega$  resonances.

| $\Omega$                 | $(v_1, v_2)$ | Mass | $\Xi\bar{K}$ | $\Xi^*\bar{K}$ | $\Omega\eta$ |
|--------------------------|--------------|------|--------------|----------------|--------------|
| ${}^2 10_{1/2}[70, 1^-]$ | (0,0)        | 1989 | 7            | –              | –            |
| ${}^2 10_{3/2}[70, 1^-]$ | (0,0)        | 1989 | 15           | –              | –            |
| ${}^4 10_{1/2}[56, 2^+]$ | (0,0)        | 2219 | 35           | 0              | –            |
| ${}^4 10_{3/2}[56, 2^+]$ | (0,0)        | 2219 | 18           | 3              | –            |
| ${}^4 10_{5/2}[56, 2^+]$ | (0,0)        | 2219 | 10           | 6              | –            |
| ${}^4 10_{7/2}[56, 2^+]$ | (0,0)        | 2219 | 43           | 5              | –            |
| ${}^2 10_{3/2}[70, 2^+]$ | (0,0)        | 2242 | 8            | 20             | 0            |
| ${}^2 10_{5/2}[70, 2^+]$ | (0,0)        | 2242 | 14           | 12             | 0            |
| ${}^2 10_J[70, 2^-]$     | (0,0)        | 2242 | 0            | 0              | 0            |
| ${}^4 10_{3/2}[56, 0^+]$ | (1,0)        | 1998 | 49           | –              | –            |
| ${}^2 10_{1/2}[70, 1^-]$ | (1,0)        | 2272 | 1            | 3              | 1            |
| ${}^2 10_{3/2}[70, 1^-]$ | (1,0)        | 2272 | 2            | 3              | 0            |
| ${}^2 10_{1/2}[70, 0^+]$ | (0,1)        | 2085 | 9            | 0              | –            |
| ${}^4 10_{1/2}[56, 1^-]$ | (0,1)        | 2306 | 109          | 4              | 0            |
| ${}^4 10_{3/2}[56, 1^-]$ | (0,1)        | 2306 | 15           | 22             | 0            |
| ${}^4 10_{5/2}[56, 1^-]$ | (0,1)        | 2306 | 90           | 15             | 0            |
| ${}^2 10_{1/2}[70, 1^-]$ | (0,1)        | 2327 | 1            | 23             | 4            |
| ${}^2 10_{3/2}[70, 1^-]$ | (0,1)        | 2327 | 1            | 19             | 3            |
| ${}^2 10_J[70, 1^+]$     | (0,1)        | 2327 | 0            | 0              | 0            |

Table XXVI: As Table XVIII, but for missing  $\Lambda^*$  resonances.

| $\Lambda^*$           | $(v_1, v_2)$ | Mass | $N\bar{K}$ | $\Sigma\pi$ | $\Lambda\eta$ | $\Xi K$ |
|-----------------------|--------------|------|------------|-------------|---------------|---------|
| $^4 1_J[20, 1^+]$     | (0,0)        | 1891 | 0          | 0           | 0             | 0       |
| $^2 1_{3/2}[70, 2^+]$ | (0,0)        | 1939 | 38         | 52          | 4             | 0       |
| $^2 1_{5/2}[70, 2^+]$ | (0,0)        | 1939 | 66         | 85          | 10            | 2       |
| $^2 1_J[70, 2^-]$     | (0,0)        | 1939 | 0          | 0           | 0             | 0       |
| $^2 1_{1/2}[70, 1^-]$ | (1,0)        | 1974 | 9          | 7           | 0             | 2       |
| $^2 1_{3/2}[70, 1^-]$ | (1,0)        | 1974 | 13         | 10          | 0             | 4       |
| $^4 1_J[20, 1^+]$     | (1,0)        | 2186 | 0          | 0           | 0             | 0       |
| $^2 1_{1/2}[70, 0^+]$ | (0,1)        | 1756 | 43         | 59          | 0             | –       |
| $^2 1_{1/2}[70, 1^-]$ | (0,1)        | 2038 | 3          | 8           | 4             | 6       |
| $^2 1_{3/2}[70, 1^-]$ | (0,1)        | 2038 | 4          | 10          | 5             | 11      |
| $^2 1_J[70, 1^+]$     | (0,1)        | 2038 | 0          | 0           | 0             | 0       |
| $^4 1_J[20, 1^-]$     | (0,1)        | 2244 | 0          | 0           | 0             | 0       |



Table XXVII: The spin-flip amplitudes of Eq. (7.5), associated with transverse helicity  $\nu = 1/2$  amplitudes for  ${}^2\delta_{1/2}[56, 0^+] \rightarrow {}^2\delta_{1/2}[56, 0^+] + \gamma$  and  ${}^4\mathbf{10}_{3/2}[56, 0^+] \rightarrow {}^2\delta_{1/2}[56, 0^+] + \gamma$  couplings with  $\mathcal{F}(k) = 1/(1 + k^2 a^2)^2$  from Table VIII. The orbit-flip amplitudes are  $\mathcal{A}_{3/2} = \mathcal{A}_{1/2} = 0$ .

| Coupling                                     | $\mathcal{B}_{1/2}$                         | $\mathcal{B}_{3/2}$                                |
|--|---|--|
| $\Sigma^0 \rightarrow \Lambda + \gamma$      | $\frac{1}{3\sqrt{3}} \mu_p \mathcal{F}(k)$  | 0  |
| $\Delta^+ \rightarrow p + \gamma$            | $-\frac{\sqrt{2}}{9} \mu_p \mathcal{F}(k)$  | $-\frac{\sqrt{2}}{3\sqrt{3}} \mu_p \mathcal{F}(k)$ |
| $\Delta^0 \rightarrow n + \gamma$            | $-\frac{\sqrt{2}}{9} \mu_p \mathcal{F}(k)$  | $-\frac{\sqrt{2}}{3\sqrt{3}} \mu_p \mathcal{F}(k)$ |
| $\Sigma^{*,+} \rightarrow \Sigma^+ + \gamma$ | $\frac{\sqrt{2}}{9} \mu_p \mathcal{F}(k)$   | $\frac{\sqrt{2}}{3\sqrt{3}} \mu_p \mathcal{F}(k)$  |
| $\Sigma^{*,0} \rightarrow \Sigma^0 + \gamma$ | $\frac{1}{9\sqrt{2}} \mu_p \mathcal{F}(k)$  | $\frac{1}{3\sqrt{6}} \mu_p \mathcal{F}(k)$         |
| $\Sigma^{*,0} \rightarrow \Lambda + \gamma$  | $-\frac{1}{3\sqrt{6}} \mu_p \mathcal{F}(k)$ | $-\frac{1}{3\sqrt{2}} \mu_p \mathcal{F}(k)$        |
| $\Sigma^{*,-} \rightarrow \Sigma^- + \gamma$ | 0   | 0  |
| $\Xi^{*,0} \rightarrow \Xi^0 + \gamma$       | $\frac{\sqrt{2}}{9} \mu_p \mathcal{F}(k)$   | $\frac{\sqrt{2}}{3\sqrt{3}} \mu_p \mathcal{F}(k)$  |
| $\Xi^{*,-} \rightarrow \Xi^- + \gamma$       | 0   | 0  |

Table XXVIII: Orbit- and spin-flip amplitudes of Eq. (7.5), associated with transverse helicity  $\nu = 1/2$  amplitudes for  ${}^2 1_J[70, 1^-] \rightarrow {}^2 8_{1/2}[56, 0^+] + \gamma$  and  ${}^2 1_J[70, 1^-] \rightarrow {}^4 10_{3/2}[56, 0^+] + \gamma$  couplings with  $\mathcal{F}(k) = i\sqrt{3}ka/(1+k^2a^2)^2$  from Table VIII and  $\mathcal{G}_-$  from Eq. (5.11). The helicity  $\nu = 3/2$  amplitudes are  $\mathcal{A}_{3/2} = \mathcal{A}_{1/2}$  and  $\mathcal{B}_{3/2} = 0$ .

| Coupling                                      | $\mathcal{A}_{1/2}$                            | $\mathcal{B}_{1/2}$                        |
|---|--|--|
| $\Lambda^* \rightarrow \Lambda + \gamma$      | $\frac{1}{6\sqrt{2}} \mu_p \mathcal{G}_-(k)/g$ | $\frac{1}{6\sqrt{2}} \mu_p \mathcal{F}(k)$ |
| $\Lambda^* \rightarrow \Sigma^0 + \gamma$     | $\frac{1}{2\sqrt{6}} \mu_p \mathcal{G}_-(k)/g$ | $\frac{1}{2\sqrt{6}} \mu_p \mathcal{F}(k)$ |
| $\Lambda^* \rightarrow \Sigma^{*,0} + \gamma$ | 0  | 0  |

Table XXIX: Transition magnetic moments associated with the  ${}^28[56] \rightarrow {}^28[56] + \gamma$  and  ${}^410[56] \rightarrow {}^28[56] + \gamma$  couplings calculated with  $\mathcal{F}(k) = 1$  (I) and  $\mathcal{F}(k) = 1/(1 + k^2 a^2)^2$  (II).

| $B \rightarrow B' + \gamma$                  | $\mu_{BB'}(k)$                           | (I)    | (II)   |
|--|--|--------|--------|
| $\Sigma^0 \rightarrow \Lambda + \gamma$      | $\mu_p \mathcal{F}(k)/\sqrt{3}$          | 1.613  | 1.588  |
| $\Delta^+ \rightarrow p + \gamma$            | $2\sqrt{2} \mu_p \mathcal{F}(k)/3$       | 2.633  | 2.206  |
| $\Delta^0 \rightarrow n + \gamma$            | $2\sqrt{2} \mu_p \mathcal{F}(k)/3$       | 2.633  | 2.208  |
| $\Sigma^{*,+} \rightarrow \Sigma^+ + \gamma$ | $-2\sqrt{2} \mu_p \mathcal{F}(k)/3$      | -2.633 | -2.411 |
| $\Sigma^{*,0} \rightarrow \Sigma^0 + \gamma$ | $-\sqrt{2} \mu_p \mathcal{F}(k)/3$       | -1.317 | -1.209 |
| $\Sigma^{*,0} \rightarrow \Lambda + \gamma$  | $\sqrt{2} \mu_p \mathcal{F}(k)/\sqrt{3}$ | 2.280  | 1.952  |
| $\Sigma^{*,-} \rightarrow \Sigma^- + \gamma$ | 0  | 0.000  | 0.000  |
| $\Xi^{*,0} \rightarrow \Xi^0 + \gamma$       | $-2\sqrt{2} \mu_p \mathcal{F}(k)/3$      | -2.633 | -2.361 |
| $\Xi^{*,-} \rightarrow \Xi^- + \gamma$       | 0  | 0.000  | 0.000  |

Table XXX: Radiative decay widths of baryons in keV. Systematic and statistical errors are added quadratically.

| $B \rightarrow B' + \gamma$                         | $\Gamma(B \rightarrow B' + \gamma)$ |           |         |                       |
|---|-------------------------------------|-----------|---------|-----------------------|
|   | Ref. [41]                           | Ref. [42] | Present | Exp.                  |
| $\Sigma^0 \rightarrow \Lambda + \gamma$             |                                     |           | 8.6     | $8.6 \pm 1.0$ [37]    |
| $\Delta^+ \rightarrow p + \gamma$                   | $430 \pm 150$                       | 350       | 343.7   | $672 \pm 56$ [13]     |
| $\Delta^0 \rightarrow n + \gamma$                   | $430 \pm 150$                       | 350       | 341.5   |                       |
| $\Sigma^{*,+} \rightarrow \Sigma^+ + \gamma$        | $100 \pm 26$                        | 105       | 140.7   |                       |
| $\Sigma^{*,0} \rightarrow \Sigma^0 + \gamma$        | $17 \pm 4$                          | 17.4      | 33.9    |                       |
| $\Sigma^{*,-} \rightarrow \Sigma^- + \gamma$        | $3.3 \pm 1.2$                       | 3.6       | 0.0     |                       |
| $\Sigma^{*,0} \rightarrow \Lambda + \gamma$         |                                     | 265       | 221.3   |                       |
| $\Xi^{*,0} \rightarrow \Xi^0 + \gamma$              | $129 \pm 29$                        | 172       | 188.2   |                       |
| $\Xi^{*,-} \rightarrow \Xi^- + \gamma$              | $3.8 \pm 1.2$                       | 6.2       | 0.0     |                       |
| $\Lambda^*(1405) \rightarrow \Lambda + \gamma$      |                                     |           | 116.9   | $27 \pm 8$ [13]       |
| $\Lambda^*(1405) \rightarrow \Sigma^{*,0} + \gamma$ |                                     |           | 0.0     |                       |
| $\Lambda^*(1405) \rightarrow \Sigma^0 + \gamma$     |                                     |           | 155.7   | $10 \pm 4$ [13]       |
|   |                                     |           |         | $23 \pm 7$ [13]       |
| $\Lambda^*(1520) \rightarrow \Lambda + \gamma$      |                                     |           | 85.1    | $134 \pm 23$ [34, 38] |
|   |                                     |           |         | $33 \pm 11$ [39]      |
| $\Lambda^*(1520) \rightarrow \Sigma^{*,0} + \gamma$ |                                     |           | 0.0     |                       |
| $\Lambda^*(1520) \rightarrow \Sigma^0 + \gamma$     |                                     |           | 180.4   | $47 \pm 17$ [39]      |

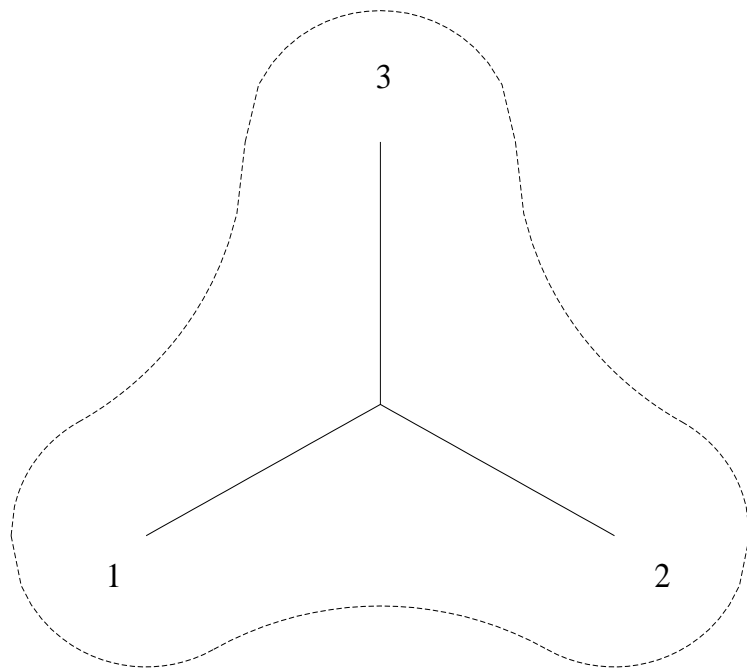


Figure 1: Collective model of baryons.

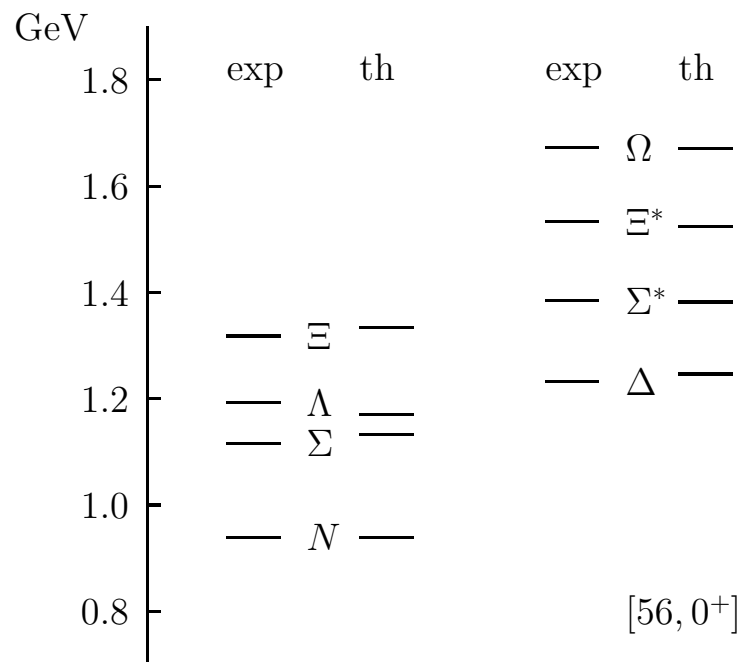


Figure 2: Ground state baryon octet with  $J^P = 1/2^+$  and decuplet with  $J^P = 3/2^+$

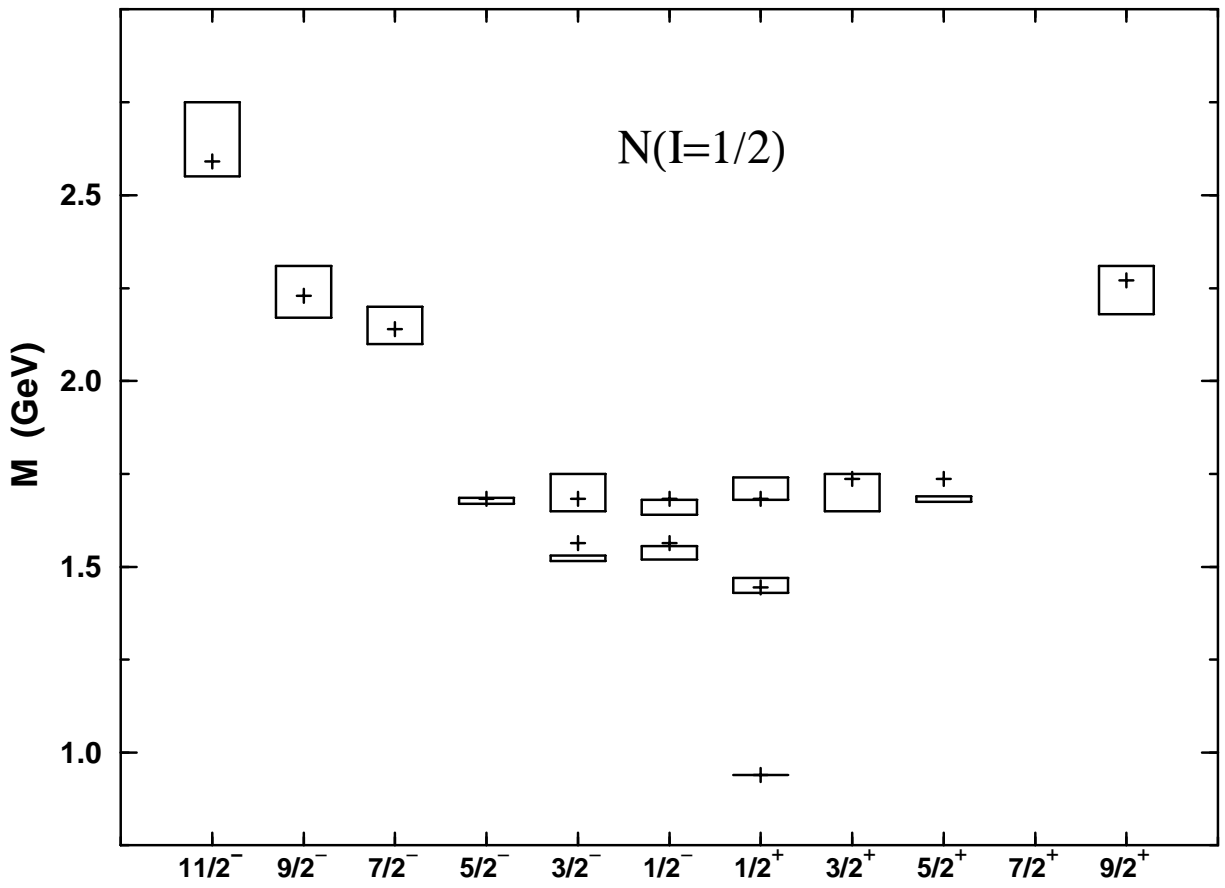


Figure 3: Comparison between the experimental mass spectrum of three and four star nucleon resonances (boxes) and the calculated masses (+).

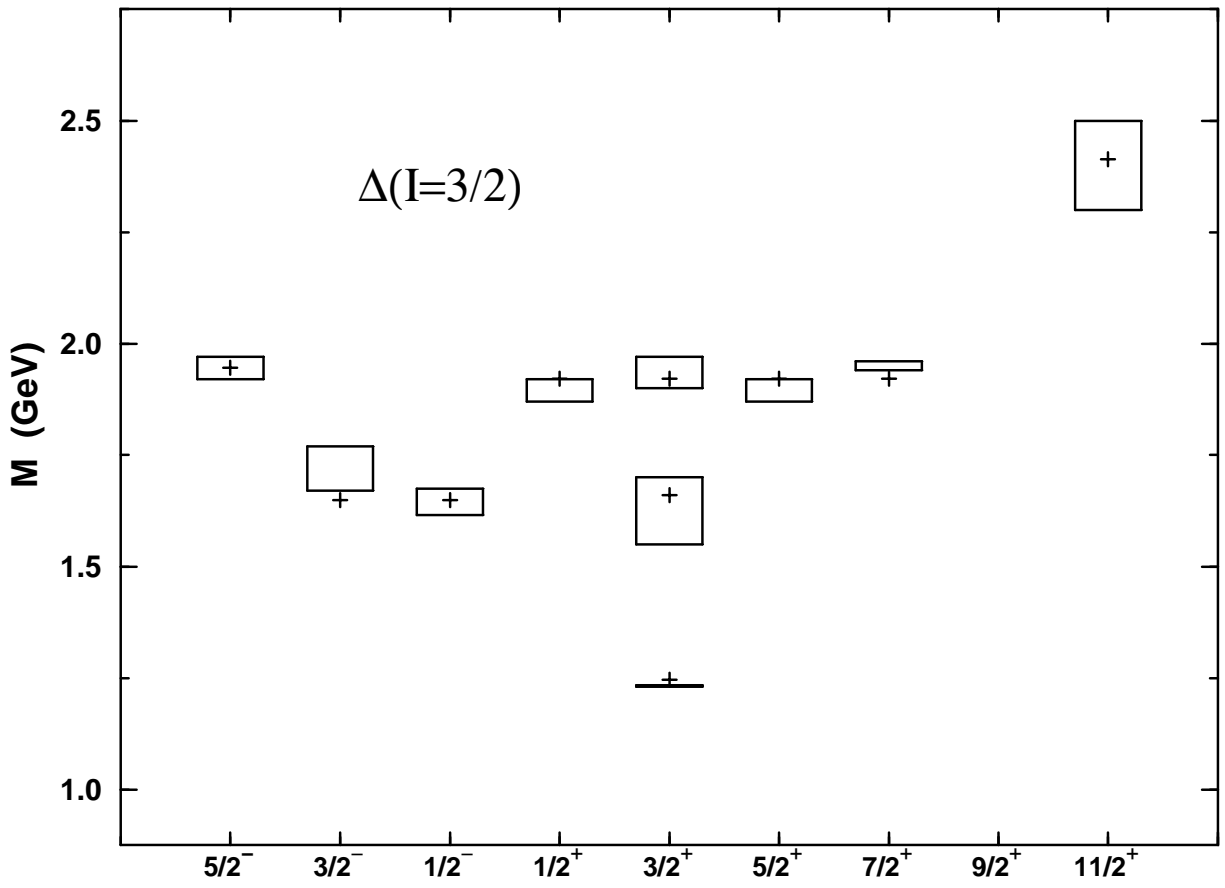


Figure 4: As Fig. 3, but for  $\Delta$  resonances.



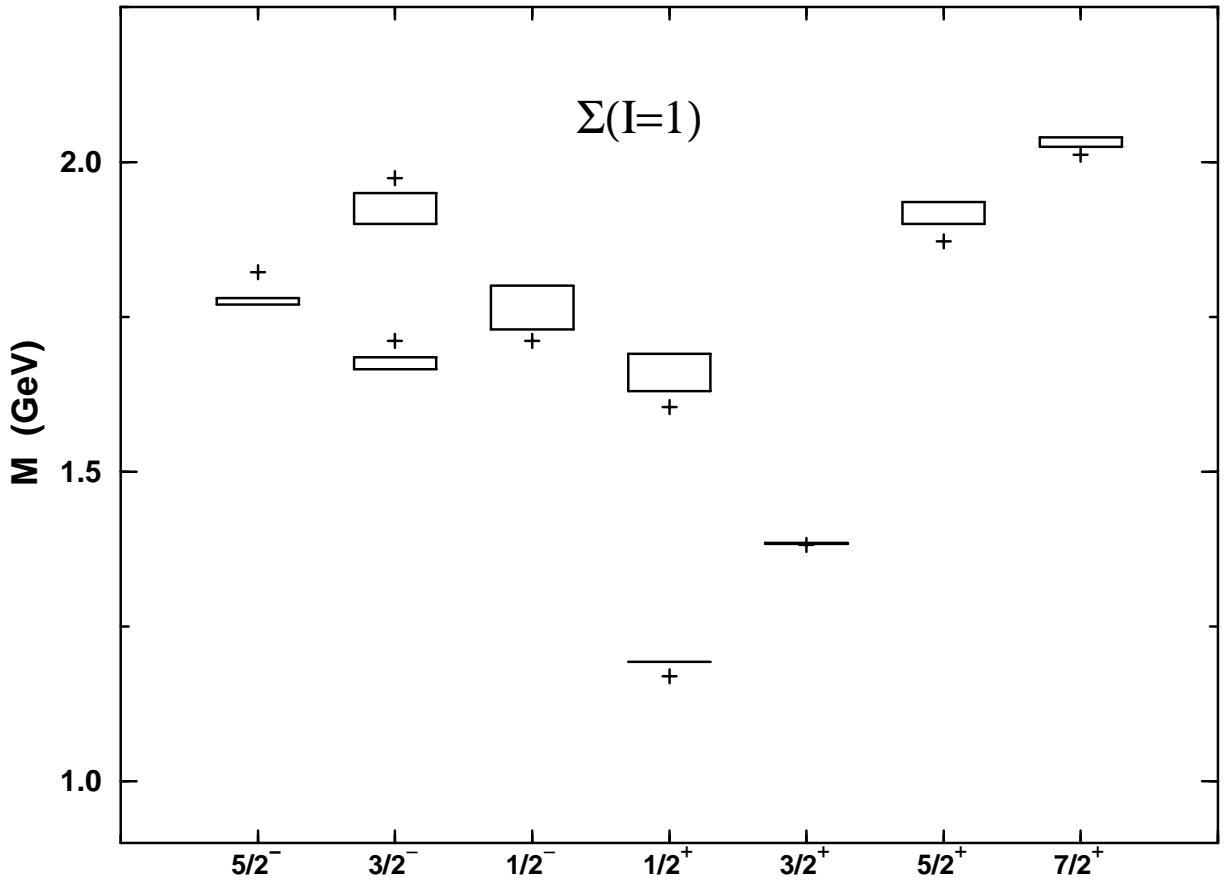


Figure 5: As Fig. 3, but for  $\Sigma$  resonances.

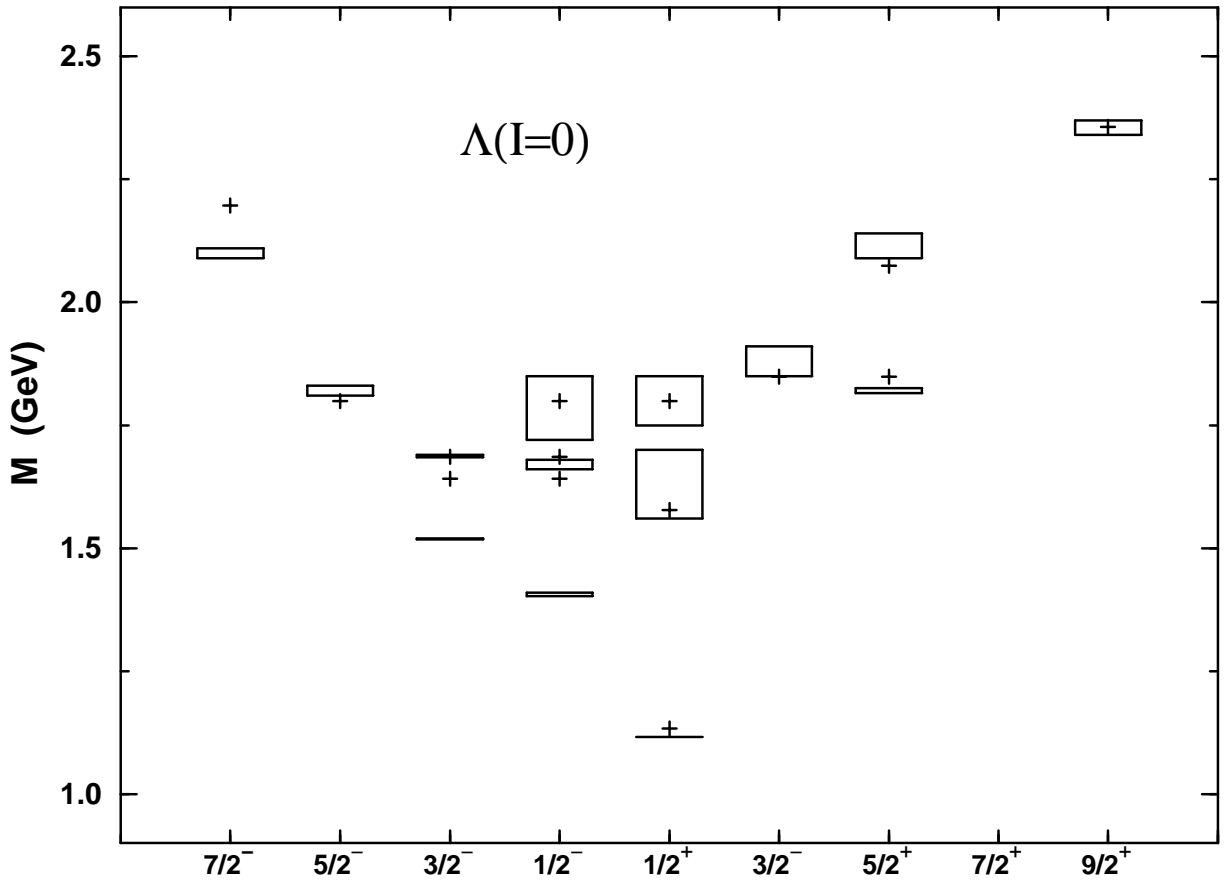


Figure 6: As Fig. 3, but for  $\Lambda$  resonances.

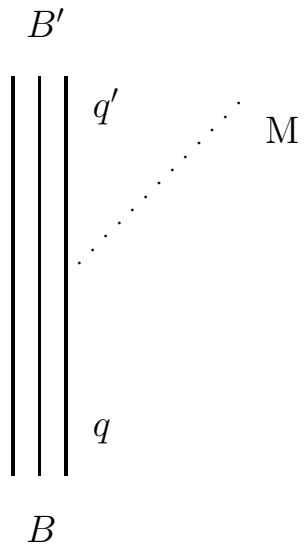


Figure 7: Elementary meson emission

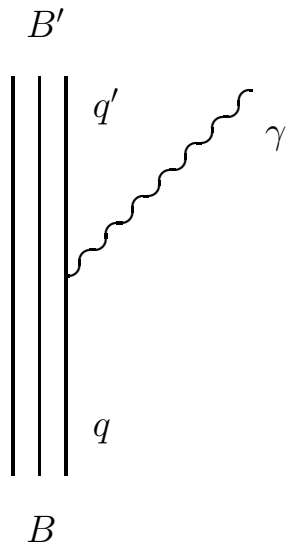


Figure 8: Photon emission